Palaeogeography, Palaeoclimatology, Palaeoecology 635 (2024) 111956

Contents lists available at ScienceDirect

Palaeogeography, Palaeoclimatology, Palaeoecology

journal homepage: www.elsevier.com/locate/palaeo

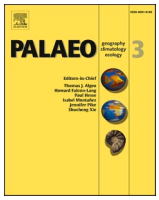

Life through an Ediacaran glaciation: Shale- and diamictite-hosted organic-walled microfossil assemblages from the late Neoproterozoic of the Tanafjorden area, northern Norway

Heda Agić [a,*], Sören Jensen [b], Guido Meinhold [c,d], Anette E.S. Högström [e], Jan Ove R. Ebbestad [f], Magne Høyberget [g], Teodoro Palacios [b], Wendy L. Taylor [h]

[a] Department of Earth Sciences, Durham University, Durham, United Kingdom
[b] Área de Paleontología, Facultad de Ciencias, Universidad de Extremadura, Badajoz, Spain
[c] Institute of Geology, TU Bergakademie Freiberg, Freiberg, Germany
[d] Department of Sedimentology and Environmental Geology, University of Göttingen, Göttingen, Germany
[e] Arctic University Museum of Norway, UiT - The Arctic University of Norway, Tromsø, Norway
[f] Museum of Evolution, Uppsala University, Uppsala, Sweden
[g] Mandal, Norway
[h] Department of Geological Sciences, University of Cape Town, Rondebosch, South Africa

ARTICLE INFO

Editor: Prof. S Shen

Keywords:
Organic-walled microfossils
Neoproterozoic
Ediacaran
Diamictite
Biostratigraphy
Palynological acid maceration

ABSTRACT

New organic-walled microfossil (OWM) assemblages are reported from upper Neoproterozoic glacial and interglacial siliciclastic deposits in Finnmark, northern Norway. A nearly continuous sedimentary succession of the Vestertana Group contains two glaciogenic units, the Smalfjorden and Mortensnes formations, interpreted as end-Cryogenian Marinoan and Ediacaran glaciations, respectively. We investigated the OWM record in the Nyborg, Mortensnes, and Stáhpogieddi formations to assess the impact of a glacial interval on the diversity of microscopic eukaryotes. A modified acid-extraction technique was applied to recover OWM from the diamictite matrix. The upper Nyborg Formation contains morphologically complex Doushantuo-Pertatataka acritarchs (DPA), restricting the age of the Nyborg Formation to early-mid Ediacaran. DPA occur below the dolostones that record a negative carbon isotope excursion correlated with the Shuram anomaly and below a glacial diamictite. A decline in species richness and compositional change is observed in the Mortensnes glacial assemblage. DPA are replaced by bacterial filaments and cell aggregates. The overlying Indreelva Member, Stáhpogieddi Formation contains Ediacara-type biota and palaeopascichnids, but only a depauperate OWM assemblage of leiosphaerids and flask-shaped microfossils characteristic of the late Ediacaran.

The succession of assemblages in the Vestertana Group demonstrates a turnover from large eukaryotic OWM to a microbial community in the glacial interval, to a low diversity post-glacial assemblage during the rise of macroscopic life. We compared the Vestertana record to global DPA occurrences. Although one DPA assemblage zone postdates the Shuram excursion, no DPA occur above Ediacaran glacial diamictites in successions where those deposits are present. Considering this, and the community changes in the Vestertana succession, we suggest that DPA were affected by the onset of an Ediacaran glaciation. Lastly, we combined the biostratigraphic markers in the Vestertana Group to constrain the age of the Mortensnes diamictite.

1. Introduction

The Ediacaran Period (635–539 Ma) is an important time in Earth's history, recording a diversification of eukaryotes, including macroscopic life, in the aftermath of severe low-latitude glaciations—the Snowball Earth events (Hoffman et al., 2017; Xiao and Narbonne, 2020). Yet it is unclear how the late Neoproterozoic glaciations facilitated biotic changes. Evidently, major eukaryotic lineages including crown groups that had evolved around the Mesoproterozoic–Neoproterozoic transition (e.g., Butterfield, 2000; Ye et al., 2015; Brocks et al., 2016; Zumberge

* Corresponding author.
E-mail address: heda.agic@durham.ac.uk (H. Agić).

https://doi.org/10.1016/j.palaeo.2023.111956
Received 27 September 2023; Received in revised form 17 November 2023; Accepted 30 November 2023
Available online 5 December 2023

et al., 2018; Sforna et al., 2022) survived through the ice-houses of the Cryogenian Period, potentially in refugia (Hoffman, 2016; Lechte et al., 2019) and even thrived during nutrient-rich, stable intervals following the post-Snowball greenhouse conditions (Bowyer et al., 2023). However, Cryogenian strata host only a depauperate fossil record (Vidal, 1976; Corsetti et al., 2003; Riedman et al., 2014; Cohen et al., 2020), in contrast to diverse older assemblages of early microeukaryotes (Cohen and Macdonald, 2015). Similarly, the diverse microfossils of the early Ediacaran (Grey, 2005; Yuan et al., 2011; Xiao et al., 2014a, 2014b; Cunningham et al., 2017) largely disappear after the Gaskiers glaciation (Zhou et al., 2007). This is unusual in comparison to modern glacial environments that house thriving microbial and even animal communities (Anesio and Laybourn-Parry, 2012; Boetius et al., 2015; Griffiths et al., 2023). In part, this could reflect preservation. Glacial and sea ice associated environments are relatively rare in the geological record, and predominantly occur as glaciogenic diamictites (Deynoux et al., 1994). However, diamictites have not been extensively investigated compared to other archives (e.g., shales) to assess changes in microfossil communities. Moreover, coarse sediments are generally ill-suited for preservation of delicate organic or skeletal fossils, leading to sampling biases (cf. Vidal, 1981; Thierstein et al., 1991) and diamictites often contain diachronous material (e.g., Streel et al., 2001). A modified microfossil-extraction technique that yields more complete microfossils and reduces contamination is used herein, to compare the microfossil record from shales and diamictites in order to examine biotic changes through late Neoproterozoic glacial and non-glacial intervals in northern Norway.

Organic-walled microfossils (OWM) represent the bulk of the Proterozoic fossil record and provide key clues about the evolution and ecology of early eukaryotic life, especially before the appearance of macroscopic organisms (Agić and Cohen, 2021). OWM with complex morphology (i.e. acanthomorphic acritarchs) rapidly diversified and reached global distribution during the early Ediacaran (e.g., Xiao and Narbonne, 2020). They occur in three different modes of preservation: phosphatization, silicification, and organic preservation in fine-grained siliciclastics. Collectively, these microfossils are called Doushantuo-Pertatataka acritarchs/microflora (DPA/DPM; Zhou et al., 2001) or Ediacaran complex acanthomorph palynoflora (ECAP; Grey et al., 2003). They have biostratigraphic potential for the subdivision and correlation of the Ediacaran system (Xiao et al., 2016; Xiao and Narbonne, 2020) and were used to establish biozones in Australia and South China (Grey, 2005; Zhou et al., 2007; Liu et al., 2013; Liu and Moczydłowska, 2019).

DPA/ECAP have also informed about the evolution of microscopic eukaryotes, and are an important component of marine environments, especially in the aftermath of severe biogeochemical and climatic perturbations. A range of biological affinities has been proposed for some DPA/ECAP taxa, including holozoan protists, green algae, and metazoans (Huldtgren et al., 2011; Chen et al., 2014; Xiao et al., 2014b; Moczydłowska, 2016; Cunningham et al., 2017). DPA/ECAP declined in the mid-late Ediacaran, around the time of the Shuram negative carbon isotope excursion (CIE) (Zhou et al., 2007; Xiao and Narbonne, 2020; Ye et al., 2023), with a few exceptions (Anderson et al., 2017; Grazhdankin et al., 2020). In a continuous succession in South China, some taxa postdate the negative CIE (Ouyang et al., 2017; Liu and Moczydłowska, 2019), but are absent in upper Ediacaran strata that otherwise record exceptional preservation of bacterial and multicellular algal fossils (Yin and Yuan, 2007; Ye et al., 2023). The late Ediacaran microfossil record is dominated by filamentous taxa and sphaeromorphs (*Leiosphaeridia*) (e.g., Leonov and Ragozina, 2007; Arvestål and Willman, 2020; Willman and Slater, 2021; Agić et al., 2022; Ye et al., 2023). The timing and drivers for the decline of DPA/ECAP taxa are not fully understood, in part due to stratigraphic incompleteness, as few sedimentary successions (outside China) preserve both lower and upper Ediacaran strata as well as glacial deposits and lithologies suitable for chemostratigraphic analyses and OWM preservation.

Here we investigated OWM occurrences through an almost continuous succession of siliciclastic sediments in the lower Vestertana Group in Finnmark, Norway (Fig. 1), including two glaciogenic diamictites (Edwards, 1984; Rice et al., 2011), to assess changes in the community composition and species richness through glacial intervals. The ages of Neoproterozoic diamictites in northern Norway recently became a source of contention based on new correlation models (Kumpulainen et al., 2021; Rice, 2023). On the grounds of their biostratigraphic utility, we use the DPA/ECAP record to further constrain the ages of glaciations in Finnmark.

2. Geological setting

2.1. Sedimentological and stratigraphic framework

The Tanafjorden area of Finnmark, northern Norway, contains a nearly continuous succession of Neoproterozoic to Lower Ordovician deposits. We investigated siliciclastic sedimentary rocks of the 1.4 km thick Vestertana Group (Fig. 1), part of the Gaissa Nappe Complex, which formed during the Caledonian Orogeny (Roberts and Gee, 1985; Meinhold et al., 2019b). The Neoproterozoic sediments on Digermulen and Varanger peninsulas in Finnmark were deposited in the north-east part of the Baltica palaeocontinent, on the Timanian margin, forming the shore of the Mirovoi superocean (Nystuen et al., 2008). In Finnmark, the Vestertana Group lies unconformably on top of the Tonian and Cryogenian Vadsø and Tanafjorden groups (Siedlecka and Siedlecki, 1971; Vidal and Siedlecka, 1983; Rice, 1994). The lower part of the Vestertana Group contains two glacial diamictites, in Smalfjorden and Mortensnes formations (Fig. 1A; Edwards, 1984; Rice et al., 2011).

Multiple Neoproterozoic glaciogenic units occur along the Caledonian margin in Norway and Sweden (e.g., Kumpulainen, 2011; Rice et al., 2001, 2011), historically referred to as the Varanger Ice Age (Kulling, 1951; Nystuen, 1985). However, the ages of these deposits, correlation of glacial units across Scandinavia, and their relationships to late Neoproterozoic Snowball Earth glaciations vary. In Finnmark, glacial diamictites have been correlated to two separate events: the Smalfjorden diamictite to the Cryogenian Marinoan glaciation (ca. 654.5–632 Ma; cf. Rooney et al., 2015) and the Mortensnes diamictite to the Ediacaran Gaskiers glaciation (ca. 579 Ma; cf. Pu et al., 2016) (Fig. 1A; Rice et al., 2011). However, an older age has also been suggested, contingent on the correlation of both units with the Marinoan Lillfjället Formation diamictites from Jämtland in Sweden (Kumpulainen et al., 2021). The upper and lower Lillfjället diamictites are cut by a dolerite dyke swarm that yielded a baddeleyite U-Pb age of 596.3 ± 1.5 Ma (Kumpulainen et al., 2021). The correlation of upper and lower Lillfjället to Smalfjorden and Mortensnes diamictites, respectively, was recently questioned by Meinhold et al. (2022), because of the required extrapolation across a distance of ca. 1000 km from Jämtland to northern Finnmark, and also dismissed by Rice (2023), because it does not fit the lithological nor $\delta^{13}C$ chemostratigraphic data characterising the Smalfjorden and Mortensnes diamictites.

The Smalfjorden Formation consists of sandstones, mudstones, conglomerates, and matrix-supported diamictites, recording several glacial advance-and-retreat cycles (Reading and Walker, 1966; Edwards, 1984; Rice et al., 2011). The upper and middle diamictites are separated by sandstone without sedimentary structures. Halverson et al. (2005) noted similarities with the Cryogenian MacDonaldryggen Member on Svalbard (below the Dracoisen Formation recently dated at 631 ± 3.8 Ma; Millikin et al., 2022). In addition, the massive cap carbonate sequence in the lower Nyborg Formation that overlies the Smalfjorden diamictite has carbonate lithology and isotopic characteristics that correlate it with other post-Marinoan cap carbonates (Edwards, 1984; Rice et al., 2001, 2011). The range of $\delta^{13}C_{carb}$ values of −2.5‰ to −4‰ in the Nyborg cap carbonate are consistent with the composite $\delta^{13}C$ record during the Marinoan glaciation and its immediate aftermath (cf. Kennedy et al., 1998; Halverson et al., 2005; He et al., 2021). Consequently, the age of

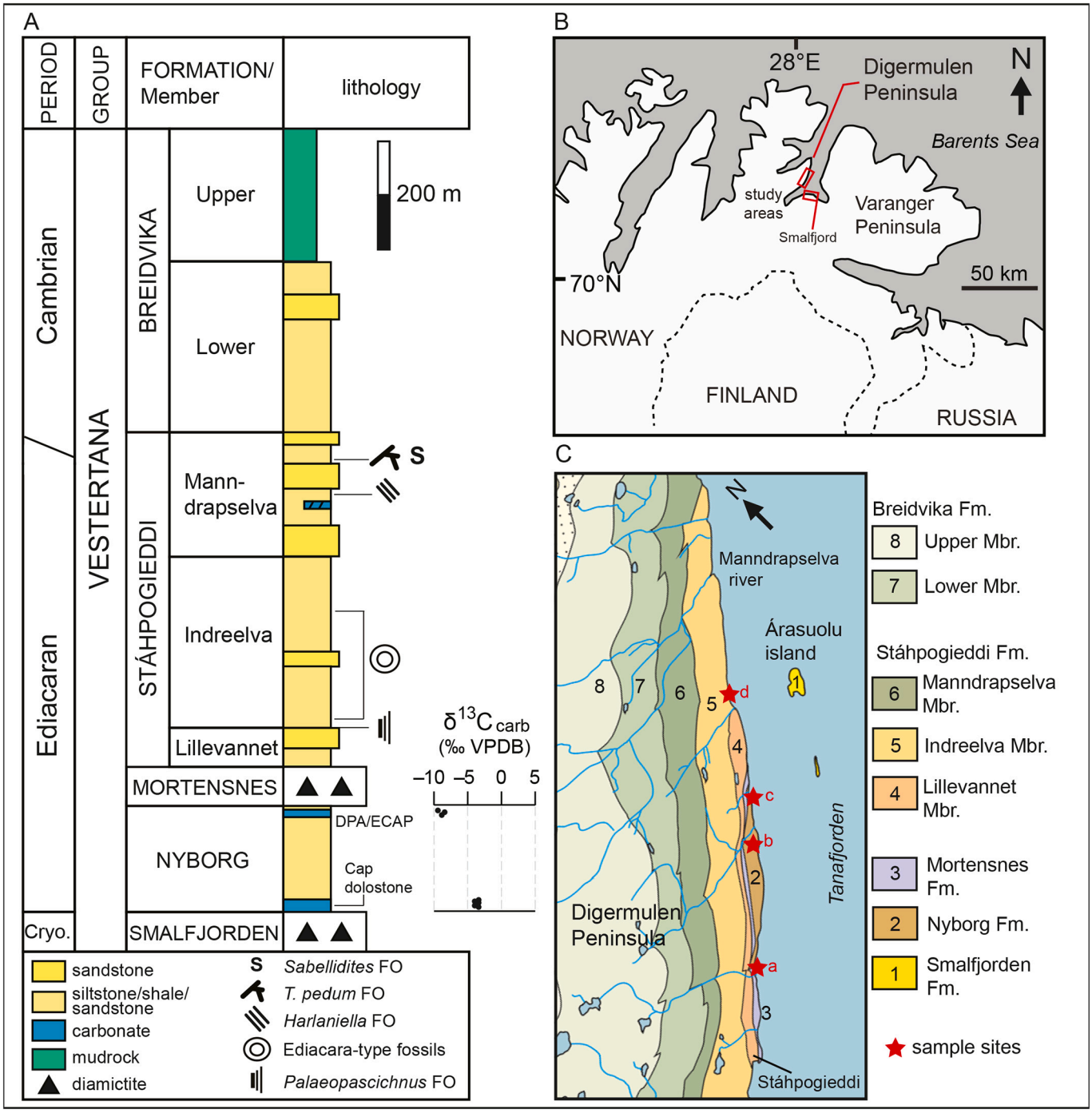

Fig. 1. Geological context and sample sites in Finnmark, northern Norway. (**A**) Simplified stratigraphy of the Cryogenian–Cambrian Vestertana Group (cf. Jensen et al., 2018), with important stratigraphic markers and local first occurrences (FO). The $\delta^{13}C$ values of the Nyborg carbonates were adapted from Halverson et al. (2005), fig. 5). (**B**) A map of northern mainland Norway, showing the position of Digermulen and Varanger peninsulas. Two study areas are marked by red squares. The majority of samples in this study are from the southeastern Digermulen Peninsula (right), and samples of the Smalfjorden Formation diamictite are from road outcrops in the Vestertana Nature Reserve area, near Smalfjord (left). (**C**) Geological units on the southeastern part of the Digermulen Peninsula (cf. Siedlecka et al., 2006). Sampling localities are marked with red stars: (a) Stáhpogieddi farm, (b) Guvssájohka gorge, (c) Nyborg cliff outcrop, (d) Árasulluokta beach. (For interpretation of the references to colour in this figure legend, the reader is referred to the web version of this article.)

the Nyborg Formation was interpreted as Ediacaran. The diamictite matrix targeted in this study is fine-grained, muddy to silty, dark purple in colour, and supports angular to subangular clasts of chert, carbonate, and quartzite (Supplementary Fig. 2B).

The Nyborg Formation is ca. 350 m thick in east Finnmark and it separates the two diamictite-bearing units (Fig. 1A; Edwards, 1984). At the base, it contains massive cap carbonates (Member A) overlain by siliciclastics of members B-D, and minor dolostones in Member E (Edwards, 1984; Rice et al., 2011). Members B-D consists of purple sandstone and dark-grey and green mudstone/siltstone packages including finely laminated shales (Banks et al., 1971; Edwards, 1984). Only the siliciclastic top part of the Nyborg Formation (Member D) is exposed on the Digermulen Peninsula, including the field localities in this study. It contains dark purple and grey-green mudstones and

siltstones interbedded with sandstone, some showing herringbone cross-bedding and lenticular bedding (Supplementary Fig. 1C). The carbonates of the topmost Member E are not exposed at our field sites. They occur only in the Gulgofjorden and Trollfjorden areas of the Varanger Peninsula, and record negative $\delta^{13}C_{carb}$ values (−9.9 to −7.6 ‰; Fig. 1A; Rice et al., 2011). The Nyborg sediments on the Digermulen Peninsula represent a shallowing-upward sequence, with a tidal influence and a development of a barrier lagoon at the top (Edwards, 1984; Rice et al., 2012). The change from the finer mudrocks of Member C to the mudstone-siltstone packages in Member D was likely a transition from a basinal, subtidal shelf environment to a shallower, tidally-influenced setting, interpreted by Edwards (1984) as a regression cycle. Previous micropalaeontological work on Nyborg Member D recovered a depauperate OWM assemblage of leiosphaerids and ornamented '*Trachysphaeridium*' (Vidal, 1981), as well as multicellular tissue fragments (Agić et al., 2019).

The Mortensnes Formation diamictite overlies the Nyborg Formation (Supplementary Fig. 1E). It varies in thickness from 10 to 50 m and contains three members: siliciclastic lower and middle members and dolomitic upper member (Edwards, 1984; Supplementary Fig. 1F). The lower member is a massive matrix-supported diamictite with varying clast size and lithology, some of which are striated (Banks et al., 1971). The middle member has dolomitic and muddy-silty matrix with common chert and basement rock clasts as well as ooid-bearing carbonate clasts (Fig. 2A–B). At the top is the dolomitic, buff-brown/yellow diamictite (Supplementary Fig. 1F). Only a thin layer (ca. 30 cm) is exposed on the Digermulen Peninsula. The lower and middle members were interpreted as glacial advance cycles, and the upper member as the retreat (Edwards, 1984). Large negative $\delta^{13}C_{carb}$ values of the dolomitic components of the diamictite were suggested to be derived from the underlying Member E of the Nyborg Formation (Rice et al., 2011). This ^{13}C-depleted signal led to a correlation of the uppermost Nyborg and Mortensnes strata with the Shuram–Wonoka $\delta^{13}C$ anomaly and a rough correlation of the Mortensnes diamictite to the Gaskiers diamictite in Newfoundland (Halverson et al., 2005; Rice et al., 2011). Vidal (1981) reported non-diagnostic OWM *Bavlinella* and *Synsphaeridium* and suggested they could have been reworked.

The Mortensnes diamictite is sharply overlain by the Stáhpogieddi Formation, a unit widely distributed across Finnmark (Reading, 1965; Banks et al., 1971; Banks, 1973). At its base is the Lillevannet Member. It is ca. 20 m thick on the Digermulen Peninsula and it contains cross-bedded and rippled sandstones, interbedded by laminated mudstones and siltstones, and quartzite at the top, representing a delta front with fluvial influence (Banks et al., 1971; Edwards, 1984). The overlying Indreelva Member is 275–300 m thick and dominated by mudstones, siltstones, siltstone lenses, and sandstones. The lower part consists of coarsening-upward cycles of grey-green shales followed by red shales and siltstones interbedded by thin, red sandstone, as well as intervals of pyritic mudstones with concretions (Supplementary Fig. 3) towards the middle part of the unit. The middle Indreelva contains green-grey mudstones and siltstones interbedded by fine-grained sandstones, occasionally showing ripples and cross-lamination representing a tidally and wave-influenced environment (Banks, 1973; Farmer et al., 1992). The upper part is laminated siltstone interbedded with thin sandstone, likely deposited in a below-wave-base environment (Banks, 1973). Macrofossils in the lower Indreelva Member on the Digermulen Peninsula include palaeopascichnids (Jensen et al., 2018), Ediacara-type fossils including discoidal taxa (Farmer et al., 1992; Högström et al., 2013; Meinhold et al., 2022) and dickinsoniamorphs (Högström et al., 2017). The lowest occurrences of palaeopascichnids are in the transition between the Lillevannet and Indreelva members (Supplementary Fig. 2D; Jensen et al., 2018). The macrofossil record and age constraints on similar assemblages imply deposition of the Indreelva sediments at 565–550 Ma (cf. Jensen et al., 2018; Kolesnikov et al., 2018; Soldatenko et al., 2019; Kolesnikov and Desiatkin, 2022). A depauperate OWM assemblage was reported from the Indreelva Member on the Varanger Peninsula (Vidal, 1981), as well as on the Digermulen Peninsula close to the first occurrence of *Palaeopascichnus* where it includes rare flask-shaped microfossils and *Granomarginata* (Agić et al., 2022).

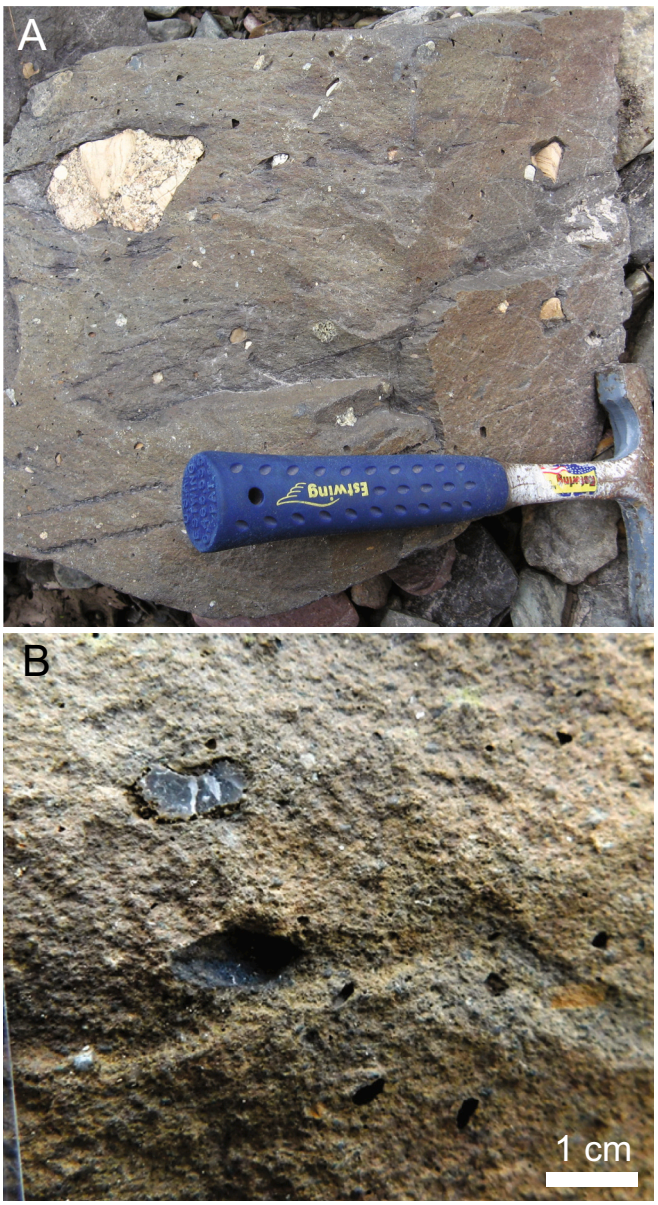

Fig. 2. Diamictites from the Vestertana Group contain fine-grained matrix. (**A**) Variable clasts in the mudstone matrix of the Mortensnes Formation diamictite. (**B**) Small chert clasts embedded in the fine-grained matrix can be manually removed during maceration to minimize or prevent contamination from older material.

The topmost part of the Vestertana Group is the Manndrapselva Member. It consists of ca. 190 m of mudstone and fine sandstone, and three quartzitic bands forming three parasequences/cycles (Reading, 1965; Banks et al., 1971; McIlroy and Brasier, 2017; Meinhold et al., 2019a, 2019b). The Ediacaran–Cambrian boundary is marked by trace fossils (including *Treptichnus pedum*) and the carbonaceous metazoan *Sabellidites cambriensis* (Högström et al., 2013; McIlroy and Brasier, 2017; Ebbestad et al., 2022).

2.2. Sample localities

Smalfjorden Formation. The diamictite was sampled in the Vestertana Nature Reserve area, at accessible roadcuts along Tanafjordveien, 70°

26.248′ N 027° 52.845 E (Fig. 1B, Supplementary Fig. 2A).

Nyborg and Mortensnes formations. Mudrock samples of the Nyborg and Mortensnes formations derive from several sections along the southeastern shore of the Digermulen Peninsula (Fig. 1C). The coastal area north of the Stáhpogieddi farm (site #a, N 70° 32.905′, E 28° 02.595′; Fig. 1C) contains exposures of the uppermost Nyborg Formation, the Mortensnes diamictite, and the Lillevannet and lower Indreelva members of the Stáhpogieddi Formation. Site #b is the exposure at the top of the Guvssájohka gorge (N 70° 33.451′ E 028° 04.736′). It contains siliciclastics of the upper Nyborg Formation and the Mortensnes diamictite. Site #c (N 70° 34.005′ E 028° 06.739′) is a short section exposed on the cliff/hilltop, containing the Mortensnes diamictite underlain by the mudstones of the Nyborg Formation.

Indreelva Member. Site #a contains the Lillevannet and basal Indreelva members. Site #d starts on the coastal outcrop opposite Árasuolu islet (N 70° 34.165′ E 28°07.244′; Fig. 1C). It exposes shales, siltstones, and sandstones of the basal portion of the Indreelva Member along the shore.

3. Materials and methods

3.1. Microfossil extraction

Organic-walled microfossils were recovered using two palynological acid maceration approaches. Specimens from shales and siltstones were extracted following the palynological acid-maceration procedure for large and delicate Ediacaran microfossils (Grey, 1999). Shale chips were washed in 30% hydrochloric acid (HCl) and submerged in 48% hydrofluoric acid (HF) for three days. The residue was decanted, and subsequently treated with boiling 30% HCl. The acid was decanted, and the residue filtered through 25 μm pore-size nylon mesh and stored in acetone. Centrifuging was not performed, to avoid damage to delicate and large microfossils. The residue was mounted onto glass slides for transmitted light microscopy and left uncovered so that scanning electron microscopy can also be performed. These uncovered slides were individually stored in Petri dishes.

The acid maceration technique was modified to extract microfossils

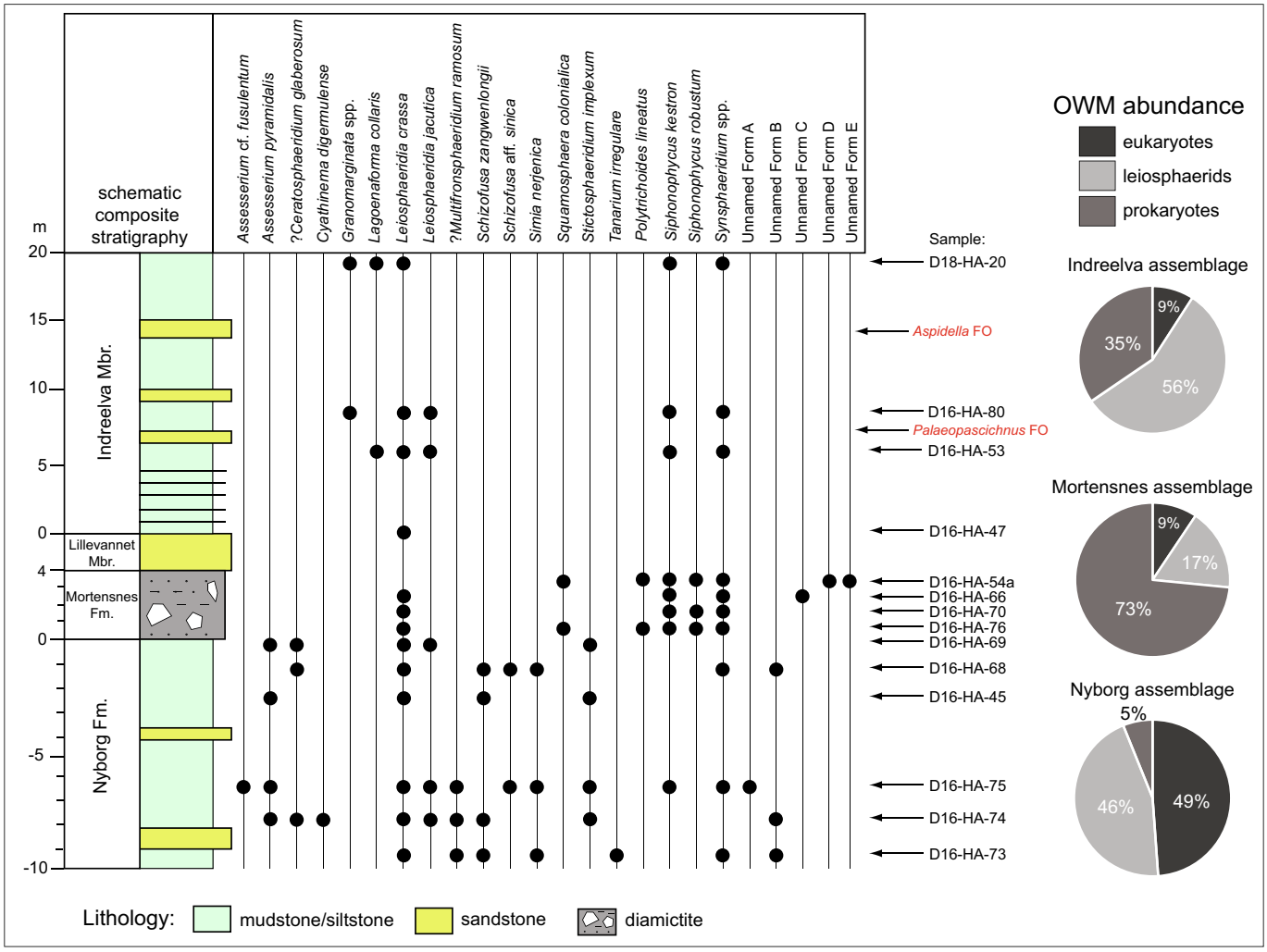

Fig. 3. Distribution of organic-walled microfossil (OWM) taxa through the lower Vestertana Group. Simplified composite stratigraphy is shown on the left (not to scale). Stratigraphic height for the Nyborg Formation is given in meters below the Mortensnes diamictite in section. Stratigraphic height for the Mortensnes Formation is given in meters above the base/contact with the Nyborg Formation in section. Stratigraphic height for the Indreelva Member of the Stáhpogieddi Formation is given in meters above the top of the non-fossiliferous Lillevannet Member. First occurrences (FO) of biostratigraphically significant macrofossils *Palaeopascichnus* and aspidellomorphs in the Indreelva Member are marked in red. Abundances of major microfossil groups (eukaryotic OWM, simple leiosphaerids, and prokaryotic filaments and cell aggregates) for each of the three investigated units is shown in pie charts on the right. The Nyborg assemblage contains a high proportion of morphologically complex OWM of eukaryotic affinity including DPA. The Mortensnes assemblage is dominated by prokaryotic taxa. The Indreelva assemblage has the lowest species richness and is dominated by leiosphaerids. The samples in the mid-upper Indreelva Member were barren. A table with abundance data for each taxon is provided in Supplementary Information (SI Table 1). (For interpretation of the references to colour in this figure legend, the reader is referred to the web version of this article.)

from diamictite intervals. Diamictite samples with fine-grained matrix (Fig. 2) were crushed into 1–2 cm pieces. Foreign clasts such as dropstones and debris were removed as much as possible. Chips of the diamictite matrix were placed in a deep, lidded Petri dish and covered with 48% HF for 24 h. As the matrix dissolved, small foreign clasts of chert and siltstone embedded in the matrix became loosened and were then carefully removed with high-density-polyethylene tweezers. This step serves to minimize contamination of the microfossil-bearing residue from sources other than the matrix itself, such as the foreign clasts. The matrix continued to be macerated in HF for another 24–48 h. The acid was decanted, and the residue washed with deionized water until neutral and then filtered through 25 μm nylon mesh, following standard palynological extraction methods (e.g., Grey, 1999).

3.2. Specimen observation and counting

Microscope observations and photography were conducted using Zeiss Axioskop transmitted light microscopes with QImaging and Leica DFC420 cameras. All illustrated specimens, as well as rock samples and glass slides with mounted fossils, are deposited in the palaeontological collection of the Arctic University Museum of Norway (UiT), prefix TSGF. Samples were collected through the non-glacial to glacial strata in several sections with the goal of observing OWM species richness changes through time, including the glacial interval. Microfossils were point-counted on one slide per sample (i.e. stratigraphic interval), which was used to determine their relative abundance (Fig. 3, Table S1).

4. Results

Nineteen taxa and four undetermined forms were recovered from 14 fossiliferous horizons in the Vestertana Group on the Digermulen Peninsula (Fig. 3, Table S1). OWM were found in the majority of processed samples from the Nyborg and Mortensnes formations (Figs. 4–6), but only in a few samples from the post-glacial Indreelva Member of the Stáhpogieddi Formation (Figs. 3, 7). Samples from the Smalfjorden Formation diamictite yielded amorphous kerogen and leiosphaerid fragments (Supplementary Fig. 4A–B). The highest diversity of microfossil taxa of eukaryotic affinity was found in the Nyborg Formation. The glacial deposits are, in contrast, dominated by prokaryotic taxa (Fig. 3). The uppermost unit included in this study, the Indreelva Member, hosts a low diversity OWM assemblage of low abundance, with only a few microeukaryotes co-occurring with macroscopic Ediacara-type biota and palaeopascichnids (Figs. 7–8).

4.1. The upper Nyborg Formation assemblage

The mudrock-hosted assemblage of the Nyborg Formation comprises prokaryotic and eukaryotic OWM taxa. Sphaeromorphs (*Leiosphaeridia*) make up nearly half of the microfossils in the assemblage (46%), but there is also a substantial component (49%) of taxa with complex morphology (Figs. 4A–D, 4I–J; Supplementary Fig. 6). These include the Doushantuo-Pertatataka acritarchs *Assesserium* cf. *fusulentum*, *A. pyramidalis*,?*Ceratosphaeridium glaberosum*, *Tanarium irregulare*, and? *Multifronsphaeridium ramosum*. Also present are the equatorial flange-bearing *Simia nerjenica* (Figs. 4E–F), and vesicles with a large split opening *Schizofusa zangwenglongii* (Figs. 4G–H), predominantly known from lower Ediacaran strata (e.g., Grey, 2005; Liu et al., 2013). Prokaryotic OWM such as simple filaments (*Siphonophycus*) and the cell aggregate *Synsphaeridium* (Figs. 4K, 5E) are present, but make up only a minor component (5%) of the assemblage (Fig. 3; Supplementary Fig. 6). Among the known regions with DPA/ECAP occurrences, the Nyborg Formation assemblage shares the most taxa with that in the Dalnyaya Tayga Group in Siberia (Table 1).

The majority of Nyborg OWM have a thermal alteration index (TAI; Marshall, 1991) of 3, indicating that the organic matter (OM) is thermally mature, but some OWM are considerably darker and duller in colour, with TAI = 5 which indicates a dry gas production window of OM maturity. The discrepancy in TAI between different OWM in the assemblage indicates that some may have been reworked.

4.2. The Mortensnes Formation diamictite assemblage

OWM from the diamictite matrix are dominated by prokaryotes (Fig. 3). Most specimens are uniform in colour (TAI = 3), although a few specimens are darker, corresponding to TAI = 4–5. This indicates different thermal or preservational histories and thus reworking, but such specimens are rare (e.g., Fig. 6J).

The most common and abundant component of the Mortensnes assemblage are *Synsphaeridium* clusters (Fig. 6E), followed by smooth-walled sphaeromorphs *Leiosphaeridia* (Figs. 6A–B). There are both indigenous (Fig. 6A) and reworked (Fig. 6B) leiosphaerids. Filamentous taxa are less common, but truncated fragments of simple filaments of varying thickness (*Siphonophycus*) are abundant in the diamictite samples. As the samples were processed with a modified low-manipulation method, the truncated nature of the specimens is less likely a result of processing and could instead be a sign of transport. Filamentous taxa also include dense, parallel, unbranched filaments *Polythrichoides lineatus* Hermann, 1974 (Fig. 6H). A single specimen of a small acanthomorph also occurs in the diamictite (Fig. 6J). The vesicle is opaque and considerably darker than the majority of the OWM assemblage, and is possibly reworked. This morphotype resembles the Ediacaran acritarch *Distosphaera australica* characterised by short, stubby processes (Grey, 2005). Toroidal morphotypes of *Squamosphaera colonialica* are also present in the Mortensens assemblage (Figs. 6F–G).

The novel OWM recovery technique from diamictites allowed recovery of more complete, less fragmented OWM. It also yielded a higher proportion of larger OWM including cell aggregates >70 μm in diameter, whilst the diamictite samples that were processed with a conventional method for extracting Precambrian microfossils by Grey (1999) yielded only small fragments of unidentifiable vesicle walls or *Synsphaeridium*, usually <20 μm in size (Supplementary Fig. 5).

4.3. The Indreelva Member assemblage

In the post-glacial succession, the lower Indreelva Member contains a depauperate OWM assemblage. The shales and siltstones of the Lillevannet Member, the lowermost unit of the Stáhpogieddi Formation, contain no OWM and only minor kerogens. The mudrocks in the lower part of the overlying Indreelva Member contain a low-abundance and low-diversity assemblage dominated by leiosphaerids (56%) and cell aggregates, as well as flask-shaped microfossils (Fig. 7). OWM occur only through the lower-mid part of the unit. The mudstones and siltstones in the middle part of the Indreelva Member are mostly red and bear pyrite crystals and concretions (Supplementary Figs. 3A–C), which indicate reducing conditions. As pyrite is formed during microbial reduction of sulphate and during degradation of organic matter (Berner, 1985), this could explain the absence of kerogen and OWM in rocks through this interval. The Indreelva Member assemblage is compositionally different from assemblages from underlying strata (Fig. 3).

5. Discussion

5.1. Preservation and reworking

Organic-walled microfossils in the upper Vestertana Group vary in preservation, from good preservation of delicate features in the Nyborg Formation Member D (cf. Agić et al., 2019) to relatively poor preservation in the Stáhpogieddi Formation, consistent with a provenance shift (Meinhold et al., 2022). Specimens of multicellular tissue *Cyathinema* and filaments in the Nyborg Formation (e.g., Fig. 5E) are mostly fragmented, even though they were extracted from the rock matrix using a gentle preparation approach, which indicates that at least some OM

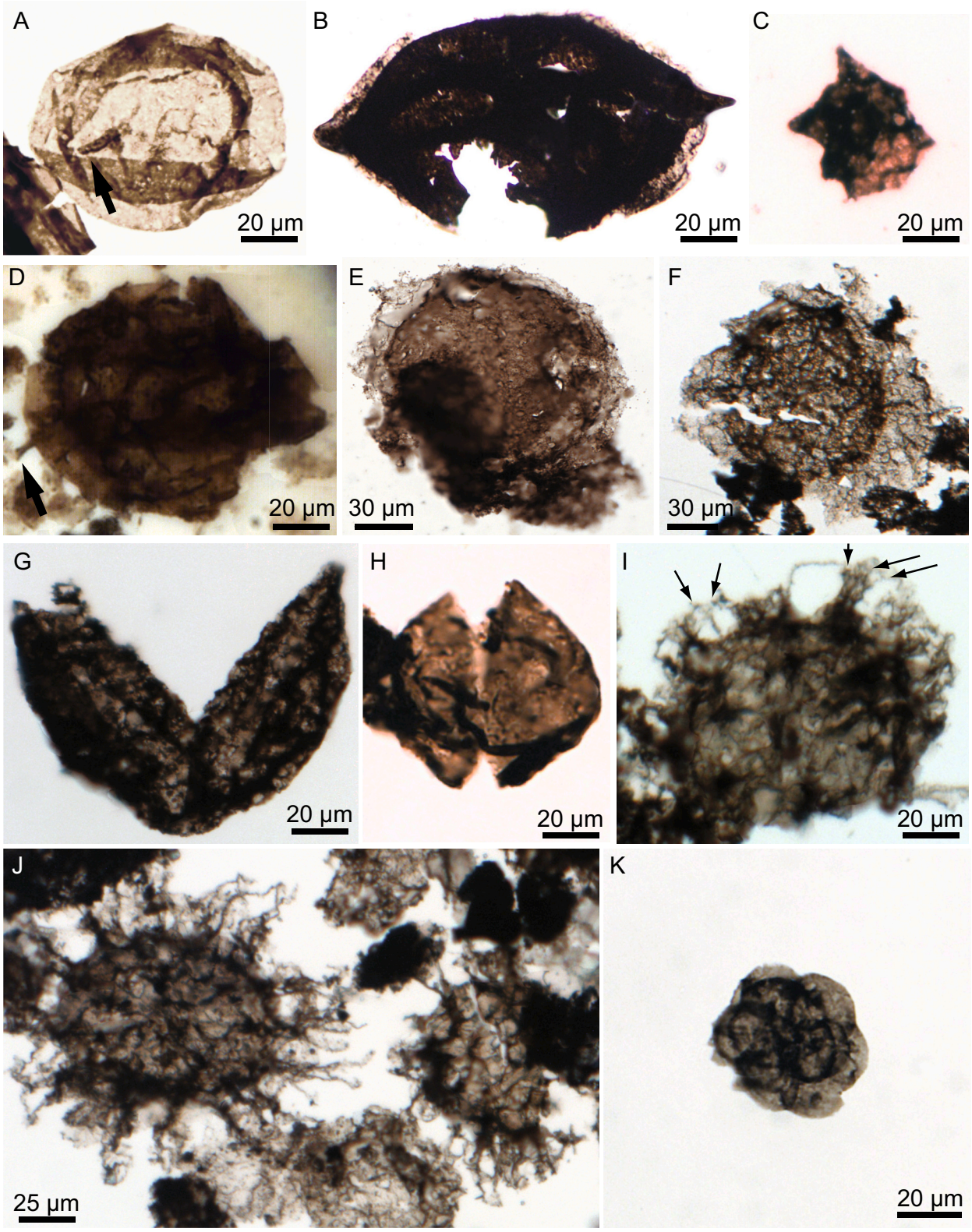

Fig. 4. Representative organic-walled microfossil taxa of the Nyborg assemblage. (**A**)?*Ceratosphaeridium glaberosum* Grey, 2005. TSGF18580a 90x6, sample D16-HA-68. The arrow points to a single process with a rounded base. (**B**) *Asseserium* cf. *fusulentum* Moczydłowska and Nagovitsin, 2012. D16-HA-75 80x12. (**C**) *Asseserium pyramidalis* Moczydłowska and Nagovitsin, 2012. TSGF18581a 98x15, D16-HA-45. (**D**) Unnamed Form A, acanthomorphs with sparse processes (indicated by the arrow). TSGF18584a 97x9.5, D16-HA-75. (**E–F**) *Simia nerjenica* Veiss in Jankauskas et al., 1989. (**E**) TSGF18583a 108x14, D16-HA-75. (**F**) TSGF18582a, sample D16-HA-73-SEM1 82x10 25×. (**G**) *Schizofusa zangwenlongii* Grey, 2005. TSGF18582b, sample D16-HA-73. (**H**) *Schizofusa* aff. *sinica* Yan, 1982. D16-HA-75-SEM2 97x9. (**I**)? *Multifronsphaeridium ramosum* Moczydłowska and Nagovitsin, 2012. TSGF18582c 87x10, D16-HA-73. Arrows show branching. (**J**) Two specimens of *Tanarium irregulare* Moczydłowska et al., 1993. TSGF18582d, TSGF18582e 108x8, D16-HA-73. (**K**) *Synsphaeridium* spp. TSFG18580b 100x9, D16-HA-68.

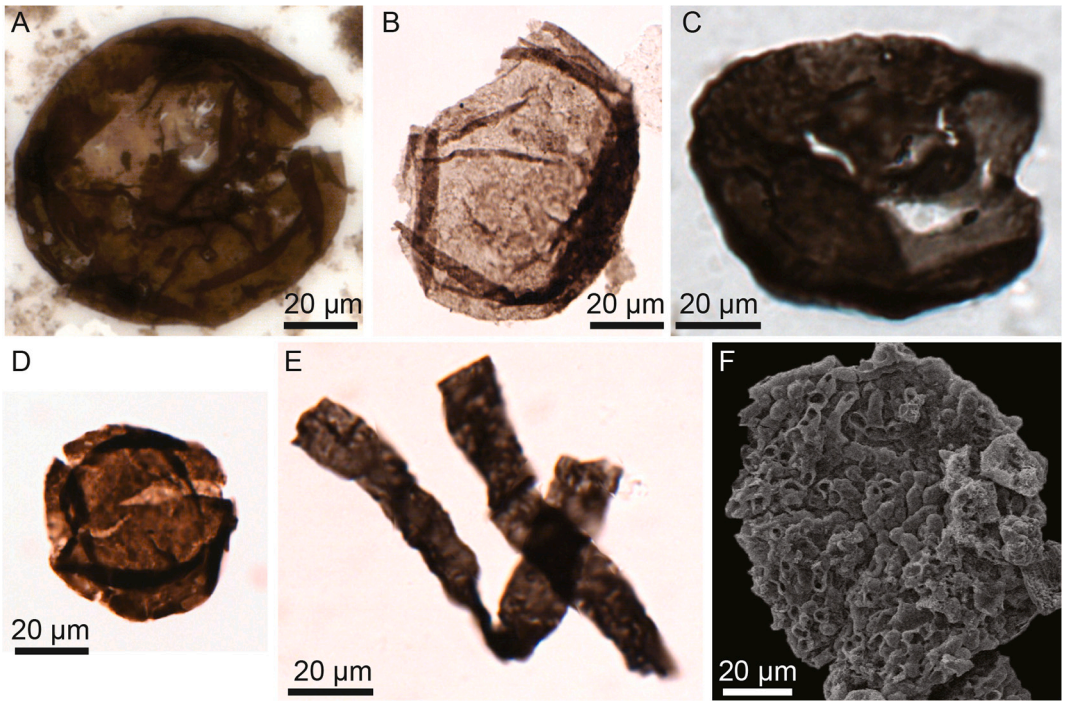

Fig. 5. Other organic-walled microfossils from the Nyborg Formation. (**A**) *Leiosphaeridia jacutica* Timofeev, 1966 emend. Mikhailova and Jankauskas in Jankauskas et al., 1989. TSGF18584b 83.5x12, D16-HA-75. (**B**) Unnamed Form B, a leiosphaerid with faintly textured vesicle wall. TSGF18580c 89x4, D16-HA-68. (**C**) *Stictosphaeridium implexum* Timofeev, 1966. TSGF18583b 77.5x14, D16-HA-75. (**D**) *Leiosphaeridia crassa* Naumova, 1949 emend. Jankauskas et al., 1989. 18584c 98x11.5, D16-HA-75. (**E**) *Siphonophycus kestron* Schopf, 1968. TSGF18583c 92.5x11, D16-HA-75. (**F**) Scanning electron photomicrograph of the tissue remains *Cyathinema digermulense* Agić et al., 2019. TSGF18423b.

was transported during or after deposition. Additionally, differences in preservation and vesicle colour between microfossils in the same assemblage indicate that some OWM may be reworked.

Allochthonous sedimentary organic matter, including OWM, is commonly reworked into autochthonous palynomorph assemblages throughout the Phanerozoic (Batten, 1991). Obvious signs of reworking include preservational and colour differences between the primary assemblage and allochthonous components. However, recognizing reworked microfossils in Proterozoic assemblages is particularly challenging because most OWM taxa have long stratigraphic ranges, so they are not easily distinguished as temporally different from the rest of the assemblage. Moreover, deep time assemblages commonly exhibit a range of preservational quality. This could reflect temporal, short-scale changes in preservational conditions, as OWM represent a death assemblage. In another rare study where OWM were recovered from glacial diamictites, in the Famennian Cabeças Formation in Brazil, the resulting assemblage of acritarchs and miospores contained 70% reworked taxa (Streel et al., 2001). Those were recognized by their older stratigraphic ranges (Givetian and Frasnian). The diamictite also contained well-preserved autochthonous taxa that confirmed the depositional environment as marine, as well as the ability of palynomorphs to become preserved in tillites (Streel et al., 2001).

We observed some signs of reworking in the present material. Several OWM in both Nyborg and Mortensnes assemblages (Figs. 4F–G, 4I–J, 6B, 6J) are duller and darker in colour than the rest of the sedimentary OM, including OWM and kerogen particles in the same samples (Figs. 4A–E, 4H, 6A, 6D, 6G–I). The rest of the acid-insoluble sedimentary OM includes scattered opaque kerogen clumps (e.g., Fig. 4J). This range of colour and, consequently, TAI values of 2–5 (cf. Staplin, 1969; Marshall, 1991) suggest that some specimens may have different thermal/depositional histories.

In a diamictite assemblage, it is possible that rare reworked specimens could derive from older mud clasts embedded in the diamictite matrix. Vidal (1981) also recovered OWM from the Mortensnes Formation on the Varanger Peninsula and suggested that all diamictite-extracted OWM must have been reworked. Vidal (1981) considered taxa like *Synsphaeridium* to derive from older rocks, because they frequently occur in older, Mesoproterozoic–Neoproterozoic assemblages. This conclusion is not supported by the fossil record, because *Synsphaeridium* is a cell aggregate form-taxon of polyphyletic nature, ranging from the Mesoproterozoic and through the Phanerozoic (Eisenack, 1965; Fensome et al., 1990) and it is present even in depauperate Cryogenian assemblages (Riedman et al., 2014) and other Ediacaran strata (e.g., Grey, 2005; Arvestål and Willman, 2020; Willman and Slater, 2021). As such, its presence in Ediacaran rocks is not unexpected. Secondly, Vidal (1981) macerated some chert nodules embedded in the Mortensnes diamictite and found that they were barren, concluding that any microfossils from the diamictite must have been reworked from older strata instead of the nodules. However, it is unclear if the chert in the Mortensnes diamictite is early diagenetic and synsedimentary with the matrix, and if it would be suited for microfossil preservation at all (cf. Manning-Berg et al., 2019). Nevertheless, if the foreign clasts are not fossiliferous and most of them have been removed through the new processing method anyway, the majority of recovered OWM come from the diamictite matrix.

The matrix-derived OWM can potentially have different origins, representing biotas inhabiting different glacial environments or even biotas transported with the till. However, in comparison with modern habitats, we would expect OWM (especially prokaryotes) in association with all glacial settings: ice, melt pools, cryoconites (e.g., Hamilton et al., 2013; Christner et al., 2014; Hancke et al., 2022). Prokaryotic taxa are delicate carbonaceous material, so it is unlikely that they would all be reworked or solely till-transported without also reworking other types of OWM (i.e. acritarchs). Based on the properties of the Vestertana material, we recognise that a few OWM from the Mortensnes diamictite could have been reworked because they stand out in colour from the rest of the acid-insoluble organics within a single sample (Figs. 6B, J), but there is no indication that the entire assemblage is reworked. On the

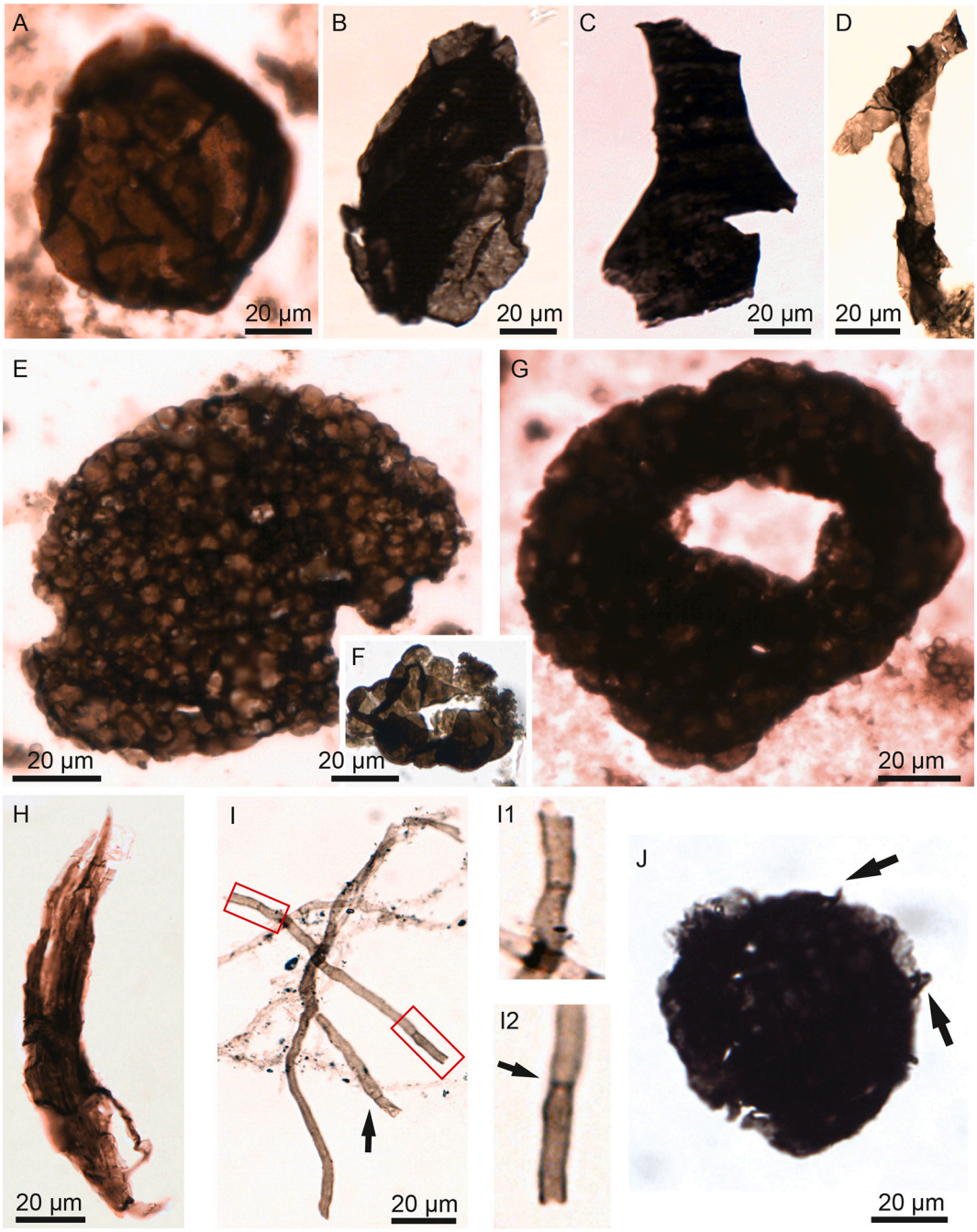

Fig. 6. Organic-walled microfossils from the Mortensnes Formation diamictite matrix. (**A**) *Leiosphaeridia crassa* Naumova, 1949. TSGF18587a 80x11, D16-HA-76. (**B**) A leiosphaerid with a *Schizofusa*-like opening. TSGF18586a 93x17, D16-HA-66. (**C**) Unnamed Form C, a fragment of a vesicle wall with striations. TSGF18586b, 94x20. (**D**) *Siphonophycus kestron* Schopf, 1968. TSGF18586c 95.5x11, D16-HA-66. (**E**) *Synsphaeridium* spp. TSGF18587b 116.5x17, D16-HA-76. (**F**) Fragment of *Squamosphaera colonialica* Jankauskas, 1979 recomb. Tang et al., 2015. TSGF18587f 93x18, D16-HA-76. (**G**) A toroidal aggregate of cells,?*Squamosphaera colonialica*. TSGF18587c 98.5x15, D16-HA-76. (**H**) *Polytrichoides lineatus* Hermann, 1974 emend. Knoll et al., 1991. TSGF18587d 87x8.5, D16-HA-76. (**I**) Unnamed Form D, septate filament. TSGF18587e 93.5x10, D16-HA-76. Red squares are enhanced in (**I1–I2**), showing the wall thickening (possible septum) in the filament. (**J**) Unnamed Form E, a small acanthomorph similar to *Distosphaera australica* Grey, 2005. TSGF18585a 87x12, D16-HA-54. It has a darker colour than other Mortensnes OWM, suggesting this could be reworked. (For interpretation of the references to colour in this figure legend, the reader is referred to the web version of this article.)

contrary, its OWM composition is prokaryote-dominant and thus distinct from the older, eukaryote-rich assemblage in the underlying Nyborg Formation (Fig. 3). This implies that the two assemblages represent different microbial communities.

The modified maceration technique used to recover the Mortensnes OWM involved picking and removing foreign clasts in the diamictite matrix during maceration to avoid contamination from older material. Despite this, it is still possible that some tiny clasts were macerated along with the matrix, or that the matrix itself contained reworked OWM due to erosion, transport, or redeposition (cf. Batten, 1991). Thus, the few darker leiosphaerids (Fig. 6B) are likely reworked, but they constitute only a minor component (2%) of Mortensnes OWM (Supplementary Fig. 6). A conspicuous reworked/darker specimen in the Mortensnes assemblage is a poorly preserved acanthomorph (Fig. 6J). Similar specimens have not been observed in older or younger strata, so its provenance is unclear. Although distinct from the Nyborg

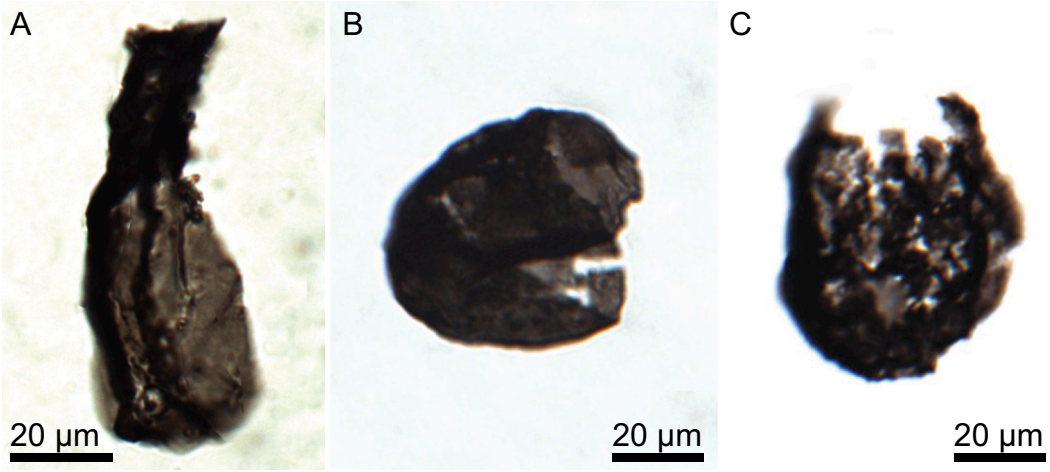

Fig. 7. Representative OWM from the depauperate post-glacial assemblage of the Indreelva Member, Stáhpogieddi Formation. (**A**) Holotype of a flask-shaped microfossil *Lagoenaforma collaris* Agić et al., 2022. TSGF18449c, D16-HA-80. (**B**) Leiosphaerid with a large opening. TSGF18588a 76x16, D16-HA-53. (**C**) Sphaeromorph with a broken vesicle. TSGF18588b 85x12, D16-HA-53.

acanthomorphs, this specimen may be classified as DPA/ECAP type. It is similar to microfossils from the Ediacaran of Siberia (Sergeev et al., 2011, fig. 7.8.) and to a specimen of *Distosphaera* from Australia in which most of the outer membrane has been lost (Grey, 2005, fig. 148C). Due to difference in colour and TAI, we consider it reworked, but it is likely not older than the Ediacaran.

Potentially reworked OWM also occur in the Nyborg shales. Acanthomorphs *Tanarium* and?*Multifronsphaeridium* have darker colour than other, more common and more abundant OWM in the assemblage (Figs. 4I–J). The two taxa occur in the lowermost sampled horizon of the Nyborg Formation (Member D), ca. 10 m below the Mortensnes diamictite (Guvssájohka section). Their exact provenance is unknown, but they are most likely reworked from the older parts of the same Nyborg Formation because 1) previous work on older units in Finnmark and elsewhere in Scandinavia did not recover DPA/ECAP (cf. Vidal, 1981; Vidal and Siedlecka, 1983; Moczydłowska et al., 2018), 2) these taxa are well age-constrained and fit with the early Ediacaran age of the Nyborg Formation, and 3) they are not significantly older than other Nyborg DPA/ECAP taxa (e.g., *Assesserium*,?*Ceratosphaeridium*, and *Schizofusa zangwenglongii*), which are also diagnostic of the early Ediacaran (cf. Grey, 2005; Zhou et al., 2007; Vorob'eva et al., 2009; Sergeev et al., 2011; Moczydłowska and Nagovitsin, 2012). Some specimens of *Simia nerjenica* (Figs. 4E–F) differ in colour within the same sample, suggesting that even if the darker OWM are reworked, they are close in age and could be a part of the same assemblage. This is consistent with the observation of sediment reworking during the regressive phase within the Nyborg Formation (Reading and Walker, 1966). The regression occurred due to a change in deposition within the same basin, so the reworked material is unlikely to be significantly older.

5.2. *Organic-walled microfossils constrain the age of the Nyborg Formation and the Vestertana Group diamictites*

5.2.1. *Early Ediacaran age of the Nyborg Formation*

The OWM assemblage from the Nyborg Formation is consistent with Doushantuo-Pertatataka acritarchs / Ediacaran complex acritarch palynoflora. These assemblages predominantly occur in strata of early Ediacaran, pre-Shuram age (Xiao, 2004) worldwide: Australia (Zang and Walter, 1992; Grey, 2005; Willman et al., 2006), Brazil (Morais et al., 2022), South China (Zhou et al., 2001, 2007; Liu et al., 2013, 2014; Xiao et al., 2014a, 2014b; Liu and Moczydłowska, 2019; Ye et al., 2022), the East European Platform (Vorob'eva et al., 2009), India (Shukla and Tiwari, 2014; Joshi and Tiwari, 2016; Prasad and Asher, 2016; Xiao et al., 2022), southern Norway (Spjeldnæs, 1967; Vidal, 1990), Siberia (Moczydłowska et al., 1993; Sergeev et al., 2011; Moczydłowska and Nagovitsin, 2012; Vorob'eva and Petrov, 2020), and Svalbard (Knoll, 1992). Exceptions of late Ediacaran acanthomorphs have been reported in China, above EN3 (Ouyang et al., 2017), Mongolia (Anderson et al., 2017), and Siberia (Golubkova et al., 2015; Grazhdankin et al., 2020). However, the ages of some of these units remain to be fully constrained, especially in Siberia, as discussed by Ye et al. (2023). Generally, upper Ediacaran strata show a lower OWM diversity, especially of acanthomorphs, and DPA/ECAP can thus be viewed as more characteristic of the early Ediacaran interval.

On Baltica, DPA/ECAP taxa also occur in the Biskopåsen Formation conglomerate, Hedmark Group in the Lake Mjøsa area in southern Norway, with acanthomorphs *Papillomembrana* and *Ericiasphaera* in chert nodules (Spjeldnæs, 1963, 1967; Vidal, 1990). *Ericiasphaera* also occurs in Ediacaran strata of Australia [Grey, 2005; although Willman et al., 2006 suggested that some specimens may belong to a new unnamed species] and south China (Zhang et al., 1998; Yuan and Hofmann, 1998; Zhou et al., 2007; Yin et al., 2011; Liu et al., 2013; Ye et al., 2022). *Papillomembrana* is also known from the lower Krol Group (Infra-Krol; Joshi and Tiwari, 2016) and Krol A Group in India (Shukla and Tiwari, 2014; Sharma et al., 2021), although Xiao et al. (2022, table 1) advised that some of these occurrences could be taphomorphs of *Appendisphaera* and need to be re-examined. Furthermore, Adamson and Butterfield (2014) reported additional DPA/ECAP in phosphorites and chert nodules in the Biskopåsen Formation and noted an overlap with the taxa in the *Tanarium conoideum* – *Hocosphaeridium scaberfacium* – *Hocosphaeridium anozos* biozone of south China (cf. Liu et al., 2014; Xiao et al., 2014a; Table 1). The Biskopåsen Formation underlies the Moelv Formation diamictite (Nystuen, 1976), which has been correlated with the Ediacaran Gaskiers diamictite contingent on lithological and geochemical properties (Kennedy et al., 1998; Halverson et al., 2005; Rice et al., 2011). This implies an early Ediacaran age of the Biskopåsen OWM. Detrital zircon U-Pb geochronology from the Rendalen Formation, significantly below the Moelv diamictite and the Biskopåsen Formation, yielded an age of 620 ± 14 Ma (Bingen et al., 2005). Rhenium-osmium (Re-Os) geochronology of the organic-rich shales underlying the Moelv diamictite yielded a 561 ± 4 Ma isochron age, suggesting that the Moelv glaciation postdates the Gaskiers (Hannah et al., 2007). These age estimates also put the timing of the deposition of the Moelv diamictite into the Ediacaran Period. The occurrence of DPA/ECAP in the uppermost Nyborg Formation (Fig. 4), just metres below the Mortensnes diamictite, supports the correlation between the Nyborg and Biskopåsen formations, and potentially the correlation of the Mortensnes and Moelv diamictites. Both localities with DPA/ECAP in

Scandinavia below glacial deposits demonstrate that Ediacaran diamictites mark the (local) decline of DPA.

It was suggested that *Papillomembrana* and *Ericiasphaera* first appeared between the Sturtian and Marinoan glaciations, implying a deeper DPA/ECAP diversification in the Cryogenian Period (Moczydłowska, 2008). However, the overlying Moelv Formation diamictite is consistent with an Ediacaran glaciation (Halverson et al., 2005), and the stratigraphic range of both taxa correspond to DPA/ECAP worldwide, so *Papillomembrana* and *Ericiasphaera* are more likely indicative of the early Ediacaran interval. Based on current known occurrences, their stratigraphic range is bracketed between the end-Cryogenian Marinoan glaciation and an Ediacaran glaciation (Gaskiers–Mortensnes–Moelv; see discussion below).

The Mortensnes diamictite overlying the DPA-bearing Nyborg assemblage contains form-taxa with long stratigraphic ranges which are not age-diagnostic. A toroidal bulbous form corresponds to *Squamosphaera colonialica* (Fig. 6G), also occurring in fragments (Fig. 6F). This is a predominantly Tonian taxon (Jankauskas et al., 1989; Tang et al., 2015), but it also occurs in the late Ediacaran of Estonia (Arvestål and Willman, 2020), so its presence in the Mortensnes Formation is not anomalous. The Mortensnes *Squamosphaera* specimens have the same colour/TAI as the majority of OWM in the assemblage, so we do not consider them to be reworked from older strata. OWM in the overlying Stáhpogieddi Formation are also not particularly age-diagnostic, although the presence of the *Granomarginata–Lagoenaforma* association points to a late Ediacaran age based on correlation with strata in Estonia, India, Iran, Namibia, and Poland (cf. Agić et al., 2022). This further supports an Ediacaran age of the Mortensnes diamictite.

Globally, the nadir of DPA/ECAP diversity appears to be before the Shuram CIE (Grey and Calver, 2007; Zhou et al., 2007; Liu et al., 2013; Ye et al., 2023). Although this anomaly has not been recorded on the Digermulen Peninsula, a large negative CIE was recorded in the topmost Nyborg Formation (Member E) on the adjacent Varanger Peninsula (Halverson et al., 2005; Rice et al., 2011). The time of the permitted duration of the Shuram CIE, according to Re-Os geochronology, postdates the Gaskiers deglaciation in Newfoundland and northwest Canada (Rooney et al., 2020). Accordingly, the DPA/ECAP microfossils of the Nyborg Formation occurring below a diamictite still fall within the global age-range of DPA/ECAP (Fig. 9) and are older than Shuram-correlative CIE as well as the Ediacaran glaciation expressed in northern Norway. It is unknown if DPA/ECAP persisted through the CIE in Member E, but they are absent from the strata overlying the excursion (Figs. 3, 9).

5.2.2. *Age of the Mortensnes Formation diamictite and implications for the mid-Ediacaran ice age*

The presence of DPA/ECAP in the Nyborg Formation also carries implications for the age of the Vestertana Group glacial diamictites. Overall, the Ediacaran age of DPA/ECAP assemblage corroborates an end-Cryogenian (Marinoan) age of the underlying Smalfjorden Formation diamictite (cf. Halverson et al., 2005; Rice et al., 2011). Consequently, the age of the Mortensnes diamictite must be younger than the end-Cryogenian Marinoan Snowball Earth glaciation (*contra* Kumpulainen et al., 2021), which broadly supports correlation with an Ediacaran glaciation (cf. Halverson et al., 2005; Rice et al., 2011; Jensen et al., 2018; Agić et al., 2022).

The upper age limit of the Mortensnes Formation diamictite is less firmly constrained (cf. Jensen et al., 2018). Due to a break in sedimentation between the Nyborg and Mortensnes formations, the diamictite could be younger than the Shuram CIE (Figs. 1A, 9). This is supported by depleted $\delta^{13}C_{carb}$ values ($< -8‰$) of the dolomite beds in the uppermost Member E of the Nyborg Formation exposed on the nearby Varanger Peninsula. These values were the basis for chemostratigraphic correlation with units expressing the Shuram CIE (Halverson et al., 2005; Rice et al., 2011; Roberts and Siedlecka, 2022). This is in contrast to the strata on Newfoundland and in NW Canada where a negative CIE postdates a short-lived glaciation (Pu et al., 2016; Rooney et al., 2020).

The occurrence of a glacial diamictite above the strata recording a Shuram-correlative CIE implies either an onset of another mid-Ediacaran glaciation after the Gaskiers glaciation and the Shuram CIE, or a diachronous nature of a single mid-Ediacaran glaciation. There are numerous Ediacaran glacial deposits worldwide (Hoffman and Li, 2009). Although many were correlated with the Gaskiers glaciation (Halverson et al., 2005; Aftabi et al., 2022), some are estimated to be younger, for instance the Kahar Formation in Iran (Etemad-Saeed et al., 2016), potentially the Granville Formation in France (Linnemann et al., 2022), and Quanji Group (Shen et al., 2010) and Hankalchough Group (Wang et al., 2023) in northwest China. These Ediacaran glaciations were not as severe as the Snowball Earth events. During the Gaskiers glaciation, the ice sheet coverage was estimated to be $>30^{\circ}$ latitude with open water at equatorial latitudes (Pu et al., 2016; Merdith et al., 2021).

Recently, a palaeogeographic reconstruction of ca. 30 Ediacaran glacial deposits and a review of their ages showed that a mid-Ediacaran glaciation was restricted to higher latitudes compared to the Snowball Earth episodes and it may have been a prolonged event spanning 580–560 Ma (Wang et al., 2023). Different ages of glacial deposits on different palaeocontinents could be a consequence of individual continents moving into higher latitudes during this interval (Wang et al., 2023). Accepting this, the Mortensnes diamictite could represent a younger end of the duration of a prolonged Ediacaran glaciation as it postdates the Shuram CIE. This interpretation is at odds with palaeocontinental reconstructions suggesting that Baltica was moving towards the equator at this time. At 600 Ma it was positioned between 55 and 75° south, and later at 560 Ma around 25–55° south (Merdith et al., 2017). Following these models, Baltica was already at relatively high latitudes and migrating northwards during the Gaskiers glaciation (ca. 580 Ma). However, a palaeocontinental reconstruction that incorporated true polar wander estimated that Baltica was positioned at high latitudes later, around 575–565 Ma (Wang et al., 2023, fig. 5), i.e. after the onset of the Gaskiers glaciation, which could explain the age discrepancy between the Mortensnes and Gaskiers diamictites. Palaeomagnetic data used for palaeocontinental reconstructions during the Ediacaran are not well constrained, including for Baltica (Domeier et al., 2023), so the relationship of the glaciation in Finnmark to the Gaskiers and other Ediacaran glaciations remains uncertain.

If the negative $\delta^{13}C$ values in the underlying Nyborg Formation truly represent the Shuram CIE, the Mortensnes Formation postdates the CIE locally. Carbonates of the Mortensnes upper member also have very negative $\delta^{13}C$ values comparable with the Shuram CIE (Rice et al., 2012, fig. 7) which could mean that the diamictite was deposited during the excursion. Rice et al. (2011) however suggested those data indicate erosion from the Nyborg Member E dolostones and redeposition in the Mortensnes upper member. In either case, based on our biostratigraphic data, the Mortensnes glaciation cannot be much younger than the Shuram CIE, and it potentially fits the permissible duration of the excursion (ca. 574–567 Ma; Rooney et al., 2020). We consider the depositional age of the Mortensnes diamictite to be approximately upper middle Ediacaran (but older than the Terminal Ediacaran Stage), because the overlying strata contain palaeopascichnids (Fig. 8A) estimated to 565 Ma or younger (Jensen et al., 2018) as well as Ediacara-type fossils (Högström et al., 2017; Meinhold et al., 2022) with the stratigraphic range around 558–550 Ma (cf. Gehling and Droser, 2013; Yang et al., 2021). If so, the Mortensnes Formation could correlate with the "Upper Ediacaran Glacial Period" (Linnemann et al., 2022) recorded from areas peripheral to northern Gondwana.

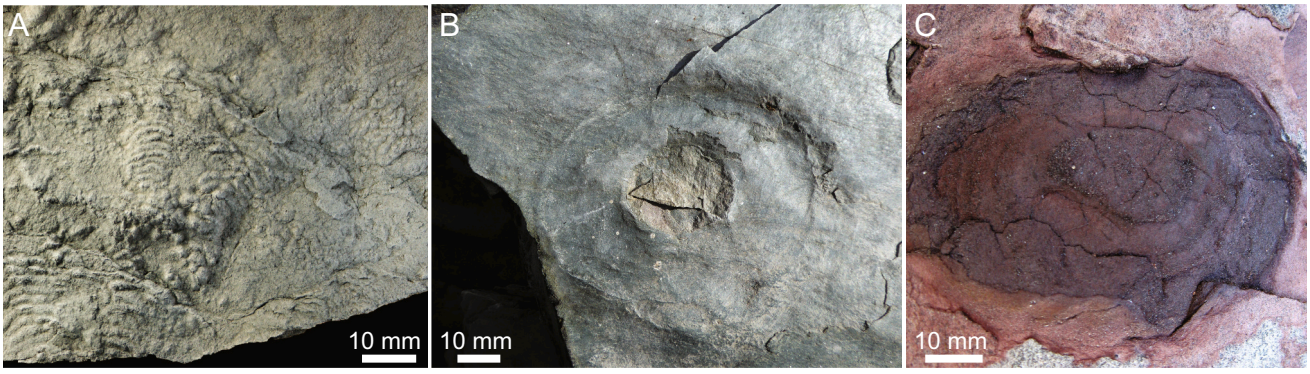

Fig. 8. Macrofossils from the Indreelva Member, Stáhpogieddi Formation, co-occurring with a depauperate OWM assemblage. (**A**) *Palaeopascichnus gracilis* Fedonkin, 1985 recomb. Kolesnikov and Desiatkin, 2022. TSGf18401. (**B-C**) Aspidellomorphs, i.e. likely holdfasts of frondose organisms. (**B**) Epirelief view. (**C**) The lowest occurrence of *Aspidella*-type discs, c. 8 m above the base of the Indreelva Member, near Stáhpogieddi farm.

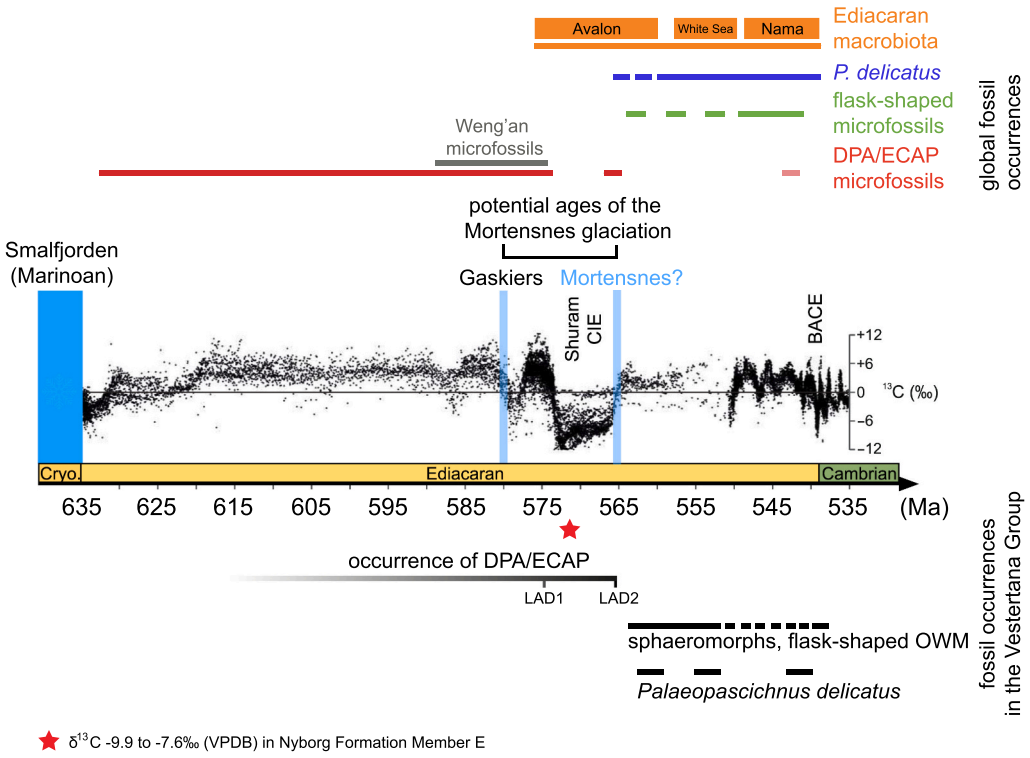

Fig. 9. Age ranges of major micro- and macrofossil types in the Ediacaran Period, in relation to the glacial intervals and a compiled $\delta^{13}C_{carb}$ profile (modified from Yang et al., 2021), including the fossil occurrences in the lower Vestertana Group in Norway. Global fossil age ranges appear in the upper part of the figure, and the inferred ranges of organic-walled microfossils and Ediacara-type biota in northern Norway are shown in the lower part. Two possibilities for the age of the Mortensnes Formation glacial diamictite based on current data are shown: it could be of Gaskiers-age (per Halverson et al., 2005), or it could postdate the Shuram CIE based on negative $\delta^{13}C_{carb}$ values in the underlying uppermost Nyborg Formation (Rice et al., 2011). In the Vestertana Group, DPA/ECAP microfossils occur in Member D of the Nyborg Formation, below the negative CIE in Member E, and below the Mortensnes diamictite. Two possible last appearance dates (LAD) from DPA/ECAP in northern Norway are: before the time of the Shuram CIE or before the onset of the Mortensnes glaciation. The strata above the diamictite contain a depauperate assemblage of sphaeromorph and flask-shaped microfossils, as well as palaeopascichnids and Ediacara-type biota (Högström et al., 2013; Jensen et al., 2018; Agić et al., 2022; Meinhold et al., 2022).

5.3. Implications for the Doushantuo-Pertatataka acritarchs' demise (or lack thereof)

On the Digermulen Peninsula, DPA/ECAP disappear during/by the Mortensnes glaciation at the latest. The overlying Stáhpogieddi Formation contains only a low-diversity assemblage with dominant leiosphaerids (Fig. 3; Agić et al., 2022). We found DPA/ECAP in the Nyborg Formation Member D. These strata are older than the Member E dolostones correlated with the Shuram CIE (Halverson et al., 2005; Rice, 2023). Fossils have not been reported from Member E, so it is unknown if DPA/ECAP occur in the CIE strata, but they are notably absent from the overlying glacial deposits as well as the younger strata. Therefore, the last appearance of DPA/ECAP in Norway is broadly marked by the Ediacaran-age diamictites, both in the case of the Biskopåsen assemblage (cf. Spjeldnæs, 1967; Vidal, 1990) and the Nyborg assemblage in this study (Fig. 9).

Globally, the stratigraphic range of DPA/ECAP is not fully constrained. Most taxa disappear around the mid-Ediacaran, more specifically around the time of or shortly after the Shuram CIE or the Gaskiers glaciation (cf. Xiao, 2004; Xiao et al., 2016; Ouyang et al., 2017; Liu and

Moczydłowska, 2019) with a few younger exceptions (Anderson et al., 2017; Anttila et al., 2021; Grazhdankin et al., 2020; see discussion by Ye et al., 2023). Reasons for this uncertainty are a lack of available units of late Ediacaran age and environments suitable for OWM preservation (cf. Grey, 2005), low sampling intensity, and the fact that few successions have the stratigraphic completeness and continuous OWM record throughout most of the Ediacaran Period. However, an increasing number of micropalaeontological studies on upper Ediacaran strata show OWM assemblages without DPA/ECAP (Volkova et al., 1983; Germs et al., 1986; Prasad et al., 2010; Jachowicz-Zdanowska, 2011; Ding et al., 2019; Arvestål and Willman, 2020; Willman and Slater, 2021; Agić et al., 2022; Środoń et al., 2023; Ye et al., 2023). This is the case even when suitable lithologies are present. The phosphorites and siliceous phosphorite nodules in the upper Ediacaran Miaohe Member, Doushantuo Formation, contain diverse microfossils of bacteria and multicellular algae, but no DPA/ECAP (Ye et al., 2023). The Vestertana Group offers a rare instance of stratigraphic coverage from the Cryogenian to the Cambrian, including the critical transitional interval in the mid-Ediacaran marked both by a glaciation and a negative CIE (Fig. 1A). Here, the OWM record exhibits a clear change in microbial communities during and after the glaciation (Fig. 3). The question remains: is this biotic turnover a global signal?

In Australia, DPA/ECAP taxa appear in lower Ediacaran strata, immediately above the Acraman impact layer (Grey et al., 2003) and disappear before ca. 565 Ma (Grey, 2005; Grey and Calver, 2007), around the end of the Shuram-Wonoka CIE (cf. Rooney et al., 2020). The strata overlying the excursion in the Wonoka Formation in south-central Australia as well as the strata overlying the Egan Formation diamictite in northwestern Australia, correlated to the Gaskiers glaciation (ca. 580 Ma; Grey and Corkeron, 1998; Corkeron and George, 2001), lack DPA/ECAP. Most upper Ediacaran deposits in Australia are sandstone-dominated, so the scarcity of fine-grained mudrocks that commonly preserve delicate OWM could explain the seeming absence of DPA/ECAP. However, where fossiliferous rocks are present, they contain leiosphaerids termed Late Ediacaran Leiosphere Palynoflora (LELP) and abundant microbialites (Grey and Corkeron, 1998; Grey, 2005), indicating a real biotic overturn.

In Brazil, DPA/ECAP (including taxa like *Assesserium* and *Tanarium* also present in the Nyborg assemblage) occur in the Bocaina Formation, Corumbá Group (Morais et al., 2022). This unit lies unconformably below the carbonates in the Tamengo Formation that record a negative CIE initially correlated with the Shuram CIE (Boggiani et al., 2010; de Oliveira et al., 2019). However, U-Pb chemical abrasion–isotope dilution–thermal ionization imaging spectrometry (CA-ID-TIMS) dating of zircons from an ash bed in the upper Bocaina Formation above the fossiliferous horizons yielded a minimum age of 555.18 ± 0.70 Ma (Parry et al., 2017), extending the stratigraphic range of DPA in southwest Brazil to upper Ediacaran. The overlying Tamengo Formation, in contrast, contains a low diversity OWM assemblage without DPA/ECAP, as well as the skeletal metazoan *Cloudina* characteristic of upper Ediacaran strata (Morais et al., 2022). The upper Ediacaran Frecheirinha Formation in northern Brazil contains a depauperate assemblage consistent with LELP (Chiglino et al., 2015). The upper Ediacaran units in the Camaquã Basin in southern Brazil also host a low-diversity OWM assemblage with prevailing sphaeromorphs and bacteria (Lehn et al., 2022). Reworked acanthomorph specimen identified as *Tanarium* has been reported from the fine-grained siliciclastics of the Santa Bárbara Group (Lehn et al., 2022, fig. 6C), but it bears straighter processes than known *Tanarium* species. Apart from that occurrence, the upper Ediacaran siliciclastics in Brazil tend to be dominated by prokaryotes, exemplified by abundant microbial textures and OWM. There are no firm age constraints on the possible glacial deposits in Brazil (cf. McGee et al., 2013), so it cannot be assessed whether DPA/ECAP were affected by a glaciation there, but the latest Ediacaran OWM record is distinctly bacteria-dominated.

In south China, DPA/ECAP are abundant in the Doushantuo Formation (e.g., Zhou et al., 2001, 2007; Liu et al., 2013, 2014; Xiao et al., 2014a). Their earliest occurrence is shortly above the Nantuo Formation diamictite corresponding to the Cryogenian Marinoan glaciation (Zhang et al., 2008). Initially, two major assemblages (*Tianzhushania spinosa* and *Tanarium anozos–Tanarium conoideum*) were recognized, separated by a negative CIE (EN2) (Liu et al., 2013). This subdivision was recently refined into four biozones. In statigraphic order, these are: *Appendisphaera grandis–Weissiella grandistella–Tianzhushania spinosa*, *Tanarium tuberosum–Schizofusa zangwenlongii*, *Tanarium conoideum–Cavaspina basiconica*, and *Tanarium pycnacanthum–Ceratosphaeridium glaberosum* assemblage zones (Liu and Moczydłowska, 2019). Only the latter assemblage occurs closely above a Shuram-correlative CIE—EN3 (Ouyang et al., 2017; Liu and Moczydłowska, 2019), but DPA/ECAP are absent from the overlying strata. Phosphorites of the uppermost Doushantuo Miaohe Member, a lithology that preserved DPA/ECAP elsewhere, contain benthic algal thalli and cyanobacterial OWM, but no acanthomorphs or biozone-diagnostic taxa (Xiao et al., 2002; Ye et al., 2023). The overlying uppermost Ediacaran Dengying Formation contains a sphaeromorph assemblage without DPA/ECAP and small acanthomorphs (<15 μm) occur only in the topmost part (Yin and Yuan, 2007). Also present are flask-shaped microfossils (Chai et al., 2021), known to occur in late Ediacaran assemblages worldwide (cf. Agić et al., 2022).

In India, DPA/ECAP are in the Infra-Krol and Krol A formations in the Lesser Himalaya (Joshi and Tiwari, 2016; Xiao et al., 2022), as well as in Sand, Lasrawan, and Khorip subgroups of the Semri Group, Lower Vindhyan (Prasad and Asher, 2016). The Infra-Krol assemblage was correlated to the *Appendisphaera grandis-Weissiella grandistella–Tianzhushania spinosa* zone in South China, and the overlying Krol A assemblage to the *Tanarium tuberosum–Schizofusa zangwenlongii* zone (Xiao et al., 2022). The latter assemblage is associated with a negative CIE corresponding to EN2 in Doushantuo Member II, and the overlying strata in Krol B-C record another CIE which has been correlated to EN3 in south China (Kaufman et al., 2006). The overlying strata lack DPA/ECAP. In the lowermost Marwar Supergroup in northern India, estimated to be of latest Ediacaran age, Prasad et al. (2010) reported a depauperate assemblage of leiosphaerids and *Granomarginata*. The Semri Group contains three DPA/ECAP assemblages, replaced by a low-diversity assemblage in the overlying Suket Shale with leiosphaerids and early Cambrian OWM.

DPA/ECAP have not been found in the Ediacaran of Iran, but OWM are present in the strata overlying glacial deposits. The Kahar Formation contains a glaciogenic diamictite constrained at 560–550 Ma with detrital zircon U-Pb geochronology (Etemad-Saeed et al., 2016). From the horizons above the diamictite, Sabouri et al. (2003) reported an OWM assemblage of leiosphaerids and flask-shaped microfossils, as well as a small carbonaceous fossil *Cochleatina* of late Ediacaran–early Cambrian age range (cf. Slater et al., 2020). The Kahar assemblage is similar to the one in the post-glacial Indreelva and Manndrapselva members of the Stáhpogieddi Formation in Norway (Fig. 3; Högström et al., 2013; Agić et al., 2022).

In the Russian Federation, DPA/ECAP taxa occur in the Barakun and Ura formations of the Dalnyaya Tayga Group in Siberia (Vorob'eva et al., 2008; Sergeev et al., 2011; Moczydłowska and Nagovitsin, 2012; Vorob'eva and Petrov, 2020) constrained to early-mid Ediacaran. Diamictites of the underlying Bol'shoy Patom Formation are overlain by a cap carbonate and estimated to be of Marinoan age (Chumakov et al., 2011; Sergeev et al., 2011). Carbonates in the Zhuya Group that overly the DPA/ECAP-bearing interval record a negative $\delta^{13}C$ excursion (around −10‰ VPDB) compatible with the Shuram anomaly (Pokrovskii et al., 2006). No Ediacaran glacial deposits are present in the Siberian succession, but the DPA/ECAP distribution is below the Shuram CIE. Pb-Pb isochron dating of limestones yielded ages of 581 ± 16 Ma below the lower microfossil horizon and 574 ± 20 Ma near the upper range (Rud'ko et al., 2021). Compositionally, the Nyborg assemblage is most similar to the Ura assemblage (Table 1) which includes

Table 1
A list of DPA/ECAP on Baltica from the Nyborg Formation (this study) and the Biskopåsen Formation (Vidal, 1990; Adamson and Butterfield, 2014) and their distribution on other palaeocontinents during the Ediacaran Period. The Nyborg assemblage is most similar to the OWM from the lower Ediacaran strata of Siberia.

Ediacaran taxa	Baltica	Australia	Brazil	China	EEP	India	Siberia	Svalbard
DPA/ECAP taxa, Nyborg Fm.								
Assesserium cf. *fusulentum*	*		*				*	
Assesserium pyramidalis	*		*		*		*	
?*Ceratosphaeridium glaberosum*	*	*		*		*	*	
?*Multifronsphaeridium ramosum*	*			*			*	
Tanarium irregulare	*	*					*	
Other non-leiosphaerid taxa, Nyborg								
Simia nerjenica	*	*		*	*	*	*	
Schizofusa zangwenlongii	*	*		*				
DPA/ECAP, Biskopåsen Fm.								
?*Appendisphaera* (Adamson & Butterfield 2014)	*	*		*			*	
?*Eotylotopalla* (Adamson & Butterfield 2014)	*		*				*	
Ericiasphaera spjeldnaesi (Vidal, 1990)	*	*						*
Papillomembrana compta (Vidal, 1990)	*							*
?*Tanarium* (Adamson & Butterfield 2014)	*	*		*	*	*	*	

A. fussulentum, *A. pyramidalis, C. glaberosum, M ramosum,* and *S. zangwenlongii*. Baltica and the Siberian Platform are estimated to have been palaeogeographically close during the Ediacaran, so it is likely that they would share some taxa.

This review of DPA/ECAP occurrences shows that the record of DPA/ECAP extends through the Shuram CIE/EN3 in some successions, but is absent from the strata bearing Ediacara-type macrofossils. And in the successions that contain glacial deposits, DPA/ECAP only occur below a diamictite. By contrast, the upper Ediacaran assemblages are usually dominated by leiosphaerids and flask-shaped microfossils (Agić et al., 2022, table 1). Rare exceptions of late Ediacaran DPA/ECAP occur in successions that record no glacial deposits (Anderson et al., 2017; Grazhdankin et al., 2020). Considering this, combined with the observation that the OWM assemblage changes in the Vestertana Group (Fig. 3), we hypothesize that DPA/ECAP were hindered by the onset of an Ediacaran glaciation. The mid-Ediacaran saw multiple short glaciations (cf. Linnemann et al., 2022) or potentially a single prolonged glacial event, manifested in the rock record at different times in the 580–560 Ma interval as different palaeocontinents travelled through cooler high latitudes (Wang et al., 2023). Both of these scenarios could partly explain why DPA/ECAP disappear at different times in different successions and why the stratigraphic ranges of some taxa/assemblages extend through the Shuram CIE/EN3 and later.

5.4. The diamictite-hosted microbiota and a biotic turnover

Prokaryotic OWM prevail in the diamictite assemblage (Fig. 3). Filamentous taxa like *Siphonophycus* were suggested to be cyanobacteria based on similarities to common modern subsection I cyanobacteria *Microcoleus chthonoplastes* (Timofeev et al., 1976) and subsection III (Oscillatoriales) (Klein et al., 1987; Lee and Golubic, 1998). Cyanobacterial affinity was also inferred for bundles of filaments *Polytrichoides* without an outer sheath (Fig. 6H) following comparison to extant "naked" multi-trichomous taxa, like *Aphanizomenon* (Supplementary Fig. 7; Lee and Golubic, 1998).

Differences between diamictite- and shale-hosted assemblages are unlikely to be an artefact of sample processing, as a modified maceration method was used that yields more complete and larger OWM (Supplementary Fig. 5). Rare studies where palynomorphs have been recovered from glaciogenic diamictites show that marine acritarchs indeed can be preserved in the matrix (Streel et al., 2001). For instance, the lower Carboniferous Jandiatuba Formation diamictite in Brazil contains a mix of reworked and autochthonous marine OWM (Caputo et al., 2008). Although the affinity of those acanthomorphic acritarchs is not constrained, their complex vesicle morphology marks them as eukaryotic. They were either benthic or dwelled in the water column under/in the ice, but in either case, they inhabited a cold environment under glacial conditions. The presence of those OWM in Carboniferous diamictites shows that eukaryotic microbiota can be preserved in glacial deposits. Thus, the absence of local acritarchs/eukaryotic OWM and good preservation of prokaryotes in the Mortensnes matrix is likely a real signal of environmental and associated biotic change.

The observed shift from a eukaryote-dominated community in the Nyborg Formation to a bacterial community (Fig. 3) suggests that prokaryotes outcompeted eukaryotic microorganisms during the glacial interval, in a changed environment. Modern glacial settings host active microbiomes, both below glacial ice sheets (Hamilton et al., 2013) and on the surface melt ponds or cryoconite holes (Cameron et al., 2012). These communities are typically dominated by bacteria and archaea (Christner et al., 2014), although eukaryotic phototrophs and heterotrophs are also an important component of modern sea ice ecosystems and often even the main contributor to primary production (Boetius et al., 2015). However, bacteria often outcompete eukaryotic primary producers in multiple environments, especially under conditions of nutrient limitation, owing to their small cell size that allows more efficient nutrient uptake (e.g., Irwin et al., 2006; Ward et al., 2014). For instance, a shift in the size of Arctic sea ice cyanobacterial and algal communities from picoplankton to larger phytoplankton (20–200 μm in diameter) occurs with increasing temperature from winter to spring time (Campbell et al., 2018). Similarly, a molecular clock analysis of a cyanobacterium *Prochlorococcus* genome, showed a population bottleneck and reduction of cell size associated with Snowball Earth glaciations (Zhang et al., 2021). Thus, the large cell size of DPA/ECAP taxa may not have been suitable for efficient nutrient uptake during the glacial regime, leading to their disappearance. Phosphorus availability is the main driver of bacterial and flagellate growth and production in modern lacustrine and glacial environments in Antarctica (Laybourn-Parry and Pearce, 2016). The low and fluctuating oxygen levels during the mid-Ediacaran (Tostevin and Mills, 2020) and redox instability brought by the glaciation would have limited bioavailable phosphorus (Van Cappellen and Ingall, 1994). Under stressful conditions such as limitation of various nutrients or temperature change, some cyanobacteria proliferate rapidly and produce toxic chemicals in the process, known as harmful algal blooms (HAB) (e.g., Preußel et al., 2009; Reinl et al., 2023). These metabolite toxins are harmful to many protists and even animals (Kosiba et al., 2019). Thus, the demise of eukaryotic microbiota may not have been caused by the glaciation directly, as many protists are adapted to cold temperatures (e.g., Devos et al., 1998; Vincent et al., 2000), but either by a nutrient limitation or ecological effects like HAB brought on by the onset of the glacial regime.

Eukaryotic organisms that produced DPA/ECAP microfossils had not recovered in the aftermath of the Mortensnes glaciation; the successive OWM assemblage is of low-diversity and dominated by simple leiosphaerids (Fig. 3). Partly, this diversity decline could be a preservational artefact. A shift in the sediment provenance may have influenced the depositional setting (Meinhold et al., 2022); for instance, the Indreelva Member contains siltier intervals less suitable for OWM preservation. Red beds occur in the lower-mid part of the Indreelva Member, bearing pyritic concretions (Supplementary Fig. 3) indicative of reducing conditions. However, where OWM are present, the assemblage includes sphaeromorphs and flask-shaped microfossils, indicating a real turnover (Fig. 3). This microeukaryote diversity decline is consistent with hopane/sterane ratio data from upper Ediacaran strata elsewhere on Baltica showing a bacterially-dominated environment under oligotrophic conditions (Pehr et al., 2018).

6. Conclusions

Our micropalaeontological investigation of a nearly continuous Cryogenian–Cambrian Vestertana Group revealed the presence of distinct organic-walled microfossil assemblages. The Nyborg Formation assemblage contains DPA/ECAP taxa, the glacial Mortensnes assemblage is bacterially-dominated, and a third assemblage in the post-glacial Indreelva Member of the Stáhpogieddi Formation is depauperate, and co-occurs with the Ediacara-type macrofossils and trace fossils. The presence of DPA/ECAP in the Nyborg Formation confirms its Ediacaran age. Consequently, it corroborates the inferred Ediacaran age of the overlying Mortensnes diamictite (cf. Halverson et al., 2005; Rice et al., 2011). The upper limit on the age of the diamictite is less certain. It overlies the strata recording a negative CIE correlated with the Shuram anomaly (Rice et al., 2011; Rice, 2023), although the topmost part of the Mortensnes Formation also records negative $\delta^{13}C_{carb}$ values consistent with Shuram CIE. Additionally, the overlying Stáhpogieddi Formation contains Ediacara-type biota with 558–550 Ma age range (Högström et al., 2013, 2017; Meinhold et al., 2022), and palaeopascichnids estimated to be younger than 565 Ma (Jensen et al., 2018). Global occurrences of these fossils indicate that the upper limit on the age of the Mortensnes diamictite is likely before ca. 560 Ma (cf. Jensen et al., 2018). Thus, the Mortensnes partly overlaps with the duration of the Shuram CIE and could represent a separate glaciation postdating the Gaskiers glaciation.

Additionally, we assessed biotic changes through this critical interval. Biases that might result from comparing assemblages in different lithologies were minimized using a new, modified palynological preparation method for extracting microfossils from glaciogenic diamictites. The recovery of OWM from the diamictite matrix allowed an insight into the environmental disturbance to the biosphere caused by a late Neoproterozoic glaciation. The Mortensnes glacial assemblage shows a shift from eukaryote-rich to a prokaryote-dominated community (Fig. 3). DPA/ECAP are also absent in the post-glacial strata that contain the oldest macroscopic Ediacara-type fossils and traces in Scandinavia. The post-glacial OWM assemblage is relatively depauperate, a characteristic of the upper Ediacaran strata (cf. Agić et al., 2022; Ye et al., 2023). Thus, based on the evidence from Norwegian units compared to the global record, we suggest that an Ediacaran glaciation led to the decline of DPA/ECAP, at least locally. Although some DPA/ECAP persist through the duration of the Shuram CIE and into younger time, they are absent above the Ediacaran glacial strata where those are preserved.

7. Systematic palaeontology

Genus *Asseserium* Moczydłowska and Nagovitsin, 2012.

Type species. *Asseserium diversum*Moczydłowska and Nagovitsin, 2012.

Asseserium cf. *fusulentum* Moczydłowska and Nagovitsin, 2012

Fig. 4B

cf. 1992 *Leiofusa bicornuta*; Zang and Walter, p. 286, pl. 7, fig. K.

cf. 2009 *Galeasphaeridium bicorporis*; Vorob'eva et al., figs. 10.6–10.10.

cf. 2012 *Asseserium fusulentum*; Moczydłowska and Nagovitsin, p. 13, figs. 5E–F.

cf. 2022 *Asseserium fusulentum*; Morais et al., fig. 5B.

Material. One specimen and a fragment from the Nyborg Formation.

Description. Ellipsoidal vesicles with bipolar symmetry, bearing two large and thick, conical processes at opposite ends. The processes taper distally, into well rounded termini. The process bases are wide, 9–11 μm in width ($N = 4$) and 9–13 μm long (N = 4). Nyborg specimens contain remnants of an outer membrane on the vesicle periphery (Fig. 4B). This membranous layer is thin, has granular texture, and is of lower opacity than the rest of the vesicle. Vesicle length (including polar processes) is 100–104 μm ($N = 2$) and the width is 60–62 μm (N = 2).

Occurrence. Lower-middle Ediacaran Ura Formation in Siberia, Russia (Moczydłowska and Nagovitsin, 2012) and Ediacaran Bocaina Formation in Brazil (Morais et al., 2022), but specimens with an outer membrane have not been reported elsewhere.

Remarks. These microfossils fall into the size range of *Assesserium fusulentum* (Moczydłowska and Nagovitsin, 2012; Morais et al., 2022). Although the Nyborg material is very similar to *A. fusulentum*, these specimens contain remnants of an outer membrane not included in the original diagnosis. It is possible that the membrane is rarely preserved. However, due to the low number of Nyborg specimens, we include these morphotypes into the genus, but only tentatively related to *A. fusulentum*. *A.* cf. *fusulentum* are also similar to *Leiofusidium dubium* (Jankauskas et al., 1989, pl. 6, figs. 1-4), an oval vesicle bearing two prong-like processes. However, the Nyborg microfossils are larger than L. *dubium* and have a thinner outer envelope, so here we assign them to *Assesserium*.

*Asseserium pyramidalis*Moczydłowska and Nagovitsin, 2012

Fig. 4C

1998 *Veryhachium* sp.; Faizullin, pl. 2, fig. 7.

2010 gen. et sp. indet.; Golubkova et al., plate IV, fig. 4.

2012 *Asseserium pyramidalis*; Moczydłowska and Nagovitsin, p. 13, fig. 5G.

Material. Three specimens from the upper Nyborg Formation.

Description. Small vesicles with short triangle-shaped processes, 26–30 μm in diameter [mean (μ) = 27 μm, standard deviation (σ) = 2.65, number of specimens (N) = 3]. The conical processes have wide bases averaging 9.5 μm in width ($\sigma = 1.9$, $N = 16$) and 6.7 μm in length ($\sigma = 1.8$, N = 16), and end in sharp tips. The processes appear to be the extensions of the vesicle wall. There are 5–6 processes on a single vesicle in the Nyborg material.

Occurrence. Upper Nyborg Formation. Lower Ediacaran Ura Formation, Urals region, Russian Federation (Moczydłowska and Nagovitsin, 2012).

Genus *Ceratosphaeridium* Grey, 2005.

Type species. *Ceratosphaeridium mirabile*Grey, 2005.

?*Ceratosphaeridium glaberosum* Grey, 2005.

Fig. 4A

Material. Three specimens from the uppermost Nyborg Formation.

Description. Circular to oval, smooth-walled vesicles with a single, prominent process, slightly tapering distally. Its base is round. The Nyborg vesicles are 65–79 μm ($N = 3$) in diameter. Processes are 16–20 μm (N = 3) long.

Occurrence. *C. glaberosum* is common in the lower Ediacaran strata worldwide, including Officer and Amadeus basins in Australia (Grey, 2005; Willman et al., 2006; Willman and Moczydłowska, 2008), Khorip Group (Lower Vindhyan) in Rajasthan, India (Prasad and Asher, 2016); Ura Formation in Siberia, Russia (Golubkova et al., 2010); Doushantuo

Formation in south China (Liu et al., 2013).

Remarks. The Nyborg specimens are on the smaller end, but within the size range of the *C. glaberosum* type material from Australia (Grey, 2005).

Genus *Cyathinema* Agić et al., 2019.

Type species. *Cyathinema digermulense*Agić et al., 2019.

*Cyathinema digermulense*Agić et al., 2019.

Fig. 5F

2019 *Cyathinema digermulense*; Agić et al., p. 2–4, figs. 1–3.

cf. 2020 "multicellular organisms"; Ye et al., p. 7, figs. 5A–F.

Material. Six specimens from the upper Nyborg Formation in Norway.

Description. Carbonaceous, rectangular to cigar-shaped forms, arranged in sheets. The fossils occur as fragments. They are composed of stacked tubes with circular openings ('cups') on one end, and vary in size and shape, as well as the number of tubes.

Occurrence. Ediacaran Nyborg Formation in Arctic Norway and potentially in the Ediacaran–Cambrian transition in the Liuchapo Formation in south China (Ye et al., 2020).

Remarks. Multicellular tissues from the Liuchapo Formation, China have been compared to *C. digermulense* (Ye et al., 2020), and share similar pseudoparenchymatous morphology under a transmitted light microscope. However, those fossils have not been extracted from the rock matrix, so the individual components of the fossil are not visible for comparison. The surface of a kerogenized multicellular alga *Elainabella deepspringensis* from the Ediacaran–Cambrian Deep Spring Formation in Nevada, USA (Rowland and Rodriguez, 2014, figs. 3.3.–3.4.) contains thallus-like elongate elements and a reticulate pattern interpreted to be cellular structure. This broadly resembles the top-down surface of *C. digermulense* fragments (cf. Fig. 5F), however, *Elainabella* occurs on the bedding plane and no material has been isolated for in-depth study of its morphology.

Genus *Multifronsphaeridium* Zang, 1992 emend. Grey, 2005

Type species. *Multifronsphaeridium pelorium* Zang in Zang and Walter, 1992.

?*Multifronsphaeridium ramosum* Moczydłowska and Nagovitsin, 2012.

Fig. 4I

cf. 2008 *Dicrospinasphaera* sp.; Vorob'eva et al., figs. 2e, j.

cf. partim 2010 *Multifronsphaeridium pelorium* Zang in Zang et Walter; Golubkova et al., p. 370, pl. 4, fig. 7.

cf. 2011 *Dicrospinasphaera virgata*; Sergeev et al., p. 996, figs. 8.1–8.5.

cf. 2012 *Multifronsphaeridium ramosum*; Moczydłowska and Nagovitsin, p. 17, figs. 7A–C.

non 2012 *Multifronsphaeridium ramosum*; Moczydłowska and Nagovitsin, p. 17, figs. 7D–F.

Material. Two specimens and a fragment in the Nyborg Formation.

Description. Circular to oval vesicles with heteromorphic processes. The vesicles are 102 and 110 μm in diameter. The processes are 14–22 μm long ($N = 13$), have wide bases (10–17 μm, $N = 13$), and branch distally. The branching is irregular. The processes appear hollow.

Occurrence. Nyborg Formation (this study) and the lower Ediacaran Ura Formation, Russian Federation (Vorob'eva et al., 2009; Golubkova et al., 2010; Sergeev et al., 2011; Moczydłowska and Nagovitsin, 2012).

Remarks. We tentatively include the Nyborg material into *Multifronsphaeridium* due to similarity with specimens from the Ura Formation, originally called *Dicrospinasphaera virgata* (Sergeev et al., 2011) and subsequently included into a new taxon *M. ramosum* (Moczydłowska and Nagovitsin, 2012). The type material of *D. virgata* from the Tanana Formation in Australia is larger, up to 220 μm in diameter, with narrower processes (Grey, 2005, figs. 140–141) than the specimens in both Ura and Nyborg formations. The processes of *D. virgata* were described as solid with straight bases (Grey, 2005, fig. 43) and not in communication with the vesicle interior, unlike the processes in similar taxa *Variomargosphaeridium litoschum* and *Multifronsphaeridium pelorium* (e.g., Grey, 2005, fig. 44). *D. virgata* (now *M. ramosus*) in the Ura Formation have hollow processes similar to the Nyborg specimens (Fig. 4I). Following this, we agree with Moczydłowska and Nagovitsin (2012) that a new taxonomic home was needed for the Ura morphotypes. However, the new specimens of *M. ramosum* in the Ura Formation have narrower processes differing in size between the specimens and are often truncated and in fewer number than on '*D. virgata*' documented by Sergeev et al. (2011). This could be a preservational artefact or a reflection of this taxon's ecological response. For instance, process size and abundance in modern dinoflagellates can drastically vary within a single species in response to changing temperature and salinity (cf. Mertens et al., 2009). Although many OWM species are established based on subtle differences in processes morphology and size, this could lead to oversplitting. Considering that, and the limited material in this study, we include the Nyborg specimens into *M. ramosum*, but note that they are more similar to the Ura specimens initially described as '*D. virgata*' (Sergeev et al., 2011) than to other *M. ramosum* (e.g., Moczydłowska, 2016, pl. 2, figs. 1–3).

Genus *Polytrichoides* Hermann, 1974 emend. Timofeev et al., 1976

Type species. *Polythrichoides lineatus*Hermann, 1974.

*Polytrichoides lineatus*Hermann, 1974 emend. Knoll et al., 1991

Fig. 6H

Material. Four specimens in the Mortensnes Formation.

Description. Bundles of parallel, smooth, non-branching filaments tightly arranged. Individual filaments are uniform in width, 1–2 μm. The width of the filamentous bundles in the Mortensnes material is 12–18 μm ($\mu = 15.5$ μm, $\sigma = 2.6$, $N = 4$).

Occurrence. Common occurrence in terminal Mesoproterozoic to Cambrian strata worldwide.

Remarks. Timofeev et al. (1976) interpreted *Polytrichoides* as a *Microcoleus*-like oscillatorialean cyanobacterium based on strong morphological similarity. In the original diagnosis, a sheath is not mentioned, but some microfossils subsequently identified as *Polytrichoides* have an outer sheath (Li et al., 2019). The relationship between these OWM and their potential modern counterparts among the sheath-less cyanobacteria are unclear. The Mortensens specimens lack a sheath, so here we compare them other "naked" filament bundles. For example, *P. lineatus* is similar to *Aphanizomenon* bundles (Supplementary Figs. 7B-C) known to form harmful blooms under stressful environmental conditions (Preußel et al., 2009).

Genus *Schizofusa* Yan, 1982.

Type species. *Schizofusa sinica*Yan, 1982.

*Schizofusa zangwenlongii*Grey, 2005.

Fig. 4G

1992 *Schizofusa* sp. pars; Zang and Walter, p. 96, figs. 71C, E, G; non *Schizofusa* sp.; p. 96, figs. 71I.

2005 *Schizofusa zangwenlongii*; Grey, p. 190, figs. 71A–D.

2011 *Schizofusa zangwenlongii*; Sergeev et al., p. 132, fig. 9.8.

2013 *Schizofusa zangwenlongii*; Liu et al., fig. 11M.

2014 *Schizofusa zangwenlongii*; Liu et al., p. 117, 108.1–108.6.

2022 *Schizofusa zangwenlongii*; Xiao et al., p. 50, figs. 30.5.–30.6.

Material. Eight specimens from the Nyborg Formation.

Description. Fusiform vesicles with a large, median-split opening. The vesicle wall is thick and chagrinate but otherwise unornamented. The rim of the median-split opening is thick, bearing narrow lips as the edge of the split vesicle wall folded in on itself. The Nyborg vesicles are 66–110 μm in diameter ($\mu = 98.1$, $\sigma = 13.7$, $N = 8$).

Occurrence. Lower Ediacaran strata in Amadeus and Officer basins,

Australia (Grey, 2005); Doushantuo Formation, China (Liu et al., 2013; Liu and Moczydłowska, 2019); Krol A Formation in the Lesser Himalaya, India (Xiao et al., 2022); Dal'nyaya Taiga Group (Vorob'eva and Petrov, 2020) and the Ura Formation (Sergeev et al., 2011), Russia.

Remarks. The texture of the vesicle wall in *S. zangwenlongii* may be contributed to scarring from mineral growth, e.g. pyrite formation (Grey and Willman, 2009), but the walls' higher opacity suggests that *S. zangwenlongii* is distinct from other, smoother and thinner-walled members of *Schizofusa*.

Genus *Simia* Mikhailova and Jankauskas in Jankauskas et al., 1989.

Type species. *Simia simica* (Jankauskas, 1980) Jankauskas et al., 1989.

Simia nerjenica Veiss in Jankauskas et al., 1989.

Figs. 4E–F

1989 *Simia nerjenica*; Veiss in Jankauskas et al., pp. 66, 67, pl. 6, figs. 9–11.

2000 *Simia* sp.; Gnilovskaya, pl. 1, fig. 4.

2006 *Simia nerjenica*; Veis et al., pl. 4, fig. 18.

2009 *Simia nerjenica* Weiss [sic]; Vorob'eva et al., p. 190, fig. 14.7.

Material. Nine specimens in the upper Nyborg Formation.

Description. Vesicles with an uneven equatorial envelope. The most prominent feature is a central body more opaque than the envelope. Some specimens show concentric folds on the central body (Fig. 4E). The transition from the central body to the equatorial envelope is well-outlined and forms a fold, especially prominent on the right side of the specimen in Fig. 4F. The envelope is texture, with fine folds. The Nyborg vesicles range in size 97–125 μm ($\mu = 112.8$, $\sigma = 10.3$, $N = 9$). The width of the equatorial envelope is uneven, and overall ranges 10–30 μm in our material.

Occurrence. Tonian strata of Siberia (Jankauskas et al., 1989); lower Ediacaran Vychegda Formation (East European Platform) in Russian Federation (Veis et al., 2006; Vorob'eva et al., 2009); potentially in the upper Ediacaran Kotlin and Voronka formations in Estonia (Arvestål and Willman, 2020, figs. 8A–E).

Remarks. A few *S. nerjenica* specimens in the Nyborg Formation may be reworked because they have darker/duller colour (Fig. 4F) than the majority of OWM in the assemblage, including other specimens of *S. simica*. As both the autochthonous and reworked members of the same taxon co-occur in the same sample, the reworked specimens are likely not much older than the rest of the Nyborg assemblage.

Genus *Squamosphaera* Tang et al., 2015 emend. Porter and Riedman, 2016

Type species. *Squamosphaera colonialica*Jankauskas, 1979b recomb. Tang et al., 2015.

*Squamosphaera colonialica*Tang et al., 2015.

Figs. 6F–G

2015 *Squamosphaera colonialica*; Tang et al., 2015, p. 312, fig. 12A–C2, fig. 13 A–F2.

2016 *Squamosphaera colonialica*; Porter and Riedman, fig. 17, 1–7.

2020 *Squamosphaera colonialica*; Arvestål and Willman, p. 8, figs. 5Q–R.

cf. 2020 *Squamosphaera*? sp.; Arvestål and Willman, p. 8, fig. 5S.

Material. Five specimens in the diamictite matrix of the Mortensnes Formation.

Description. Elongate to toroidal vesicles, overall 60–83 μm in diameter ($\mu = 71$ μm, $\sigma = 9.3$, $N = 4$), bearing rounded, dome-like ornamentation that cover the entire vesicle. Individual ornamentation elements are visible on specimens preserved only as wall fragments; the vesicle breaks along the lines of ornamentation (Fig. 6F).

Occurrence. *S. colonialica* is predominantly known from terminal Mesoproterozoic-Tonian rocks (cf. Tang et al., 2015), and from the upper Ediacaran Kotlin Formation in Estonia (Arvestål and Willman, 2020).

Genus *Stictosphaeridium* Timofeev, 1966 emend. Mikhailova and Jankauskas in Jankauskas et al., 1989.

Type species. *Stictosphaeridium sinapticuliferum*Timofeev, 1966.

*Stictosphaeridium implexum*Timofeev, 1966.

Fig. 5C

1966 *Stictosphaeridium implexum*; Timofeev, pl. 5, fig. 5.

1974 *Stictosphaeridium implexum*; Gunia, pl. 2, fig. 5.

1982 *Stictosphaeridium implexum* Timofeev; Jankauskas, pl. 43, fig. 5.

2001 *Stictosphaeridium implexum* Timofeev; Prasad and Asher, pl. 10, figs. 10, 13.

2008 *Stictosphaeridium implexum* Timofeev; Mehrotra et al., p. 545, fig. 2c.

2017 *Stictosphaeridium sinapticuliferum*; Sergeev et al., pl. 1, fig. 14.

2017 *Stictosphaeridium implexum* Timofeev; Agić et al., p. 120, figs. 13A–C.

cf. 2020 *Stictosphaeridium sinapticuliferum*; Arvestål and Willman, p. 9, figs. 6Q–R.

Material. Seven specimens in the upper Nyborg Formation.

Description. Spheroidal to elongate vesicles, with irregular, thin, crest-like folds along the vesicle wall. The medium to dark opacity of the microfossils indicates that the vesicle wall is robust, but the fine, "pinched" folds indicate that it is also pliant. The wrinkles are broadly spread out along the vesicle surface, otherwise smooth in between the folds. The Nyborg specimens are 63–82 μm in diameter ($\mu = 73.9$ μm, $\sigma = 6.4$ μm, $n = 7$).

Occurrence. Proterozoic to Cambrian strata. In Ediacaran strata, *S. implexum* also occurs in the metasediments of the Duszniki Zdrój area in Poland (Gunia, 1974).

Remarks. Pyatiletov (1978) considered *S. implexum* to be taphomorphs of *Stictosphaeridium laccatum* that was subsequently combined with *Protoleiosphaeridium laccatum* (Fensome et al., 1990), now also an invalid genus. It is unclear whether the *S. implexum* type material has been compared and synonymized with a valid taxon, but the diagnoses and illustrations of the type material do differ (compare Timofeev, 1966, pl. 4 fig. 6 and pl. 5 fig. 5); *P. laccatum* lacks pliant folds its folds and is more similar to leiosphaerid compressions. Unfortunately, the type material has been only drawn, not photographed (Timofeev, 1966), meaning that some features could be artefacts, or missing entirely. Here, we assign specimens with a wrinkled wall to *S. implexum* based on this species' diagnosis ("narrow, crest-like, branching ornamentation"; Timofeev, 1966), as well as similarities to other *S. implexum* (e.g., Mehrotra et al., 2008; Agić et al., 2017). Clusters of sphaeromorphs "cf. *Stictosphaeridium*" were reported from the Mortensnes Formation (Vidal, 1981), as well as in the older Klubbnes and Andersby formations (Vidal, 1981, figs. 19A–F). However, those forms also include cellular inclusions and overall correspond to a cell aggregate *Synsphaeridium*.

Genus *Tanarium* Kolosova, 1991, emend. Moczydłowska et al., 1993

Type species. *Tanarium conoideum*Kolosova, 1991, emend. Moczydłowska et al., 1993.

*Tanarium irregulare*Moczydłowska et al., 1993.

Fig. 4J

1993 *Tanarium irregulare*; Moczydłowska et al., pl. 7, figs. 1–2.

2005 *Tanarium irregulare* Moczydłowska, Vidal and Rudavskaya; Grey, p. 306, figs. 220A–F, 221A-D.

2006 *Tanarium irregulare*; Willman et al., p. pl. 7, figs. 1–2.

2013 *Tanarium irregulare*; Liu et al., p. 39, fig. 11L.

cf. 2020 *Tanarium pycnacanthum* Grey; Vorob'eva and Petrov, pl. 1, figs. 10–12.

Material. Four specimens from the Nyborg Formation.

Description. Spherical to ovoid vesicles with long, hollow, thin processes with triangular bases. The vesicles (with processes) in the Nyborg material are 100–120 μm in diameter ($\mu = 109.2$ μm, $\sigma = 9.8$ μm, $n = 4$). The processes are hollow, have conical bases (around 5–10 μm wide)

and taper outwards. Termini are very thin, occasionally bifurcating. The processes vary in length on a single vesicle, typically 30–55 μm (μ = 38.8 μm, σ = 5.9 μm, *n* = 25).

Occurrence. Rare occurrence in the Nyborg Formation. *T. irregulare* is also known from: upper Neoproterozoic Khamaka Formation in Siberia, Russia (Moczydłowska et al., 1993); Ediacaran Karlaya Limestone, Australia (Grey, 2005; Willman et al., 2006).

Remarks. Genus *Tanarium* numbers a myriad species (see Xiao et al., 2022, p. 38), some of which are very similar, e.g. *T. irregulare* and *T. pycnacanthum*. As a result, the distinction is not always clear-cut, especially in poorly to moderately preserved material where processes on one specimen may be of different sizes on different sides of the vesicle (compare figs. 220 and 245 in Grey, 2005). Here, we include the Nyborg specimens into *T. irregulare* based on the shape of the processes and vesicle size. The diameter of the Nyborg OWM falls within size range of the *T. irregulare* material from Australia (52–218 μm, mean diameter 116 μm; Grey, 2005) and Siberia (75–115 μm in diameter; Moczydłowska et al., 1993). The mean diameter of the Nyborg specimens is bigger than, or on the upper end of the size range of *T. pycnacanthum* material from Australia (size range of 32–180 μm; Grey, 2005) and China (65–115 μm; Liu et al., 2014). *T. irregulare* is an index fossil of the *Tanarium irregulare–Ceratosphaeridium glaberosum–Multifronsphaeridium pelorium* (Ti/Cg/Mp) assemblage of south Australia (Grey, 2005). *T. irregulare* was reported form the Ediacaran Santa Bárbara Group in Brazil (Lehn et al., 2022, fig. 6C), but it contains scarce and broader processes than indicated by the diagnosis, so here we do not count that specimen into occurrences.

Unnamed Form A

Fig. 4D

Material. One specimen in the Nyborg Formation.

Description. Ovoid vesicle bearing scarce, thin, flaring-outwards processes. The vesicle wall in between the processes is smooth and bears numerous compression folds. The ellipsoid vesicle is 84 μm long. The processes are short and only fully visible on the outline of the specimen.

Unnamed Form B

Fig. 5B

cf. 1983 *Kildinosphaera granulata*; Vidal and Siedlecka, p. 57–58, fig. 5H–J.

cf. 2017 *Vidalopalla granulata* comb. nov.; Agić et al., pp. 106, 116, figs. 4E, 12A–G.

Material. Three specimens from the upper Nyborg Formation.

Description. Circular to elongate vesicles with low to moderate opacity, and a faintly sculptured wall. The sculpture is grainy. Diameter of the Nyborg vesicles ranges 62–65 μm (μ = 63.6 μm, σ = 1.5 μm, *n* = 3).

Remarks. The grainy sculpture could result either from the granular nature of the vesicle wall, or poor preservation from mineral growth in the vesicle wall (e.g., Grey and Willman, 2009). Considering that these morphotypes occur alongside OWM with a smooth and well-preserved vesicle wall (e.g., Fig. 6A), this particular sculpture could represent a primary feature. Unnamed Form B is similar to OWM with granular wall sculpture *Vidalopalla granulata*. This taxon was initially reported from the Tonian Klubbnes Formation on the neighbouring Varanger Peninsula (Vidal and Siedlecka, 1983, figs. 5H–J), and also occurs in the Mesoproterozoic (Prasad and Asher, 2001; Agić et al., 2017). However, the individual granulae are not clearly distinguished on the only two Nyborg specimens, and more fossils would be needed for assignment into *V. granulata*. OWM with sculpture are a common component of Mesoproterozoic and lower Neoproterozoic strata (cf. Agić and Cohen, 2021).

Unnamed Form C

Fig. 6C

Material. Two specimens form the Mortensnes Formation diamictite matrix.

Description. Carbonaceous fragments with moderate to high opacity, bearing faint striations. The fragments are sharply outlined, which indicates breakage.

Remarks. Broadly similar problematic striated fragments are present in a number of Ediacaran units (e.g., Veis et al., 2006, pl. 4, figs. 1–4), but their simple and fragmented nature precludes taxonomic assignment.

Unnamed Form D

Fig. 6I

cf. 2006 "*Stiganema*-like branching sheath"; Veis et al., p. 376, pl. 4, fig. 17.

Material. Two specimens form the Mortensnes diamictite matrix.

Description. Straight, septate filaments, around 5 μm wide, branching sideways. The branches are the same size and shape as the filaments they branch from. The filaments are divided by septa-like wall thickenings (Fig. 6I1-I2). The length of the filaments between each 'septum' (where visible) on the Mortensnes specimens is 24–38 μm (μ = 34.4 μm, σ = 5.8 μm, *N* = 5).

Remarks. Similar but wider branching filaments occur in the Ediacaran Vychegda Formation, East European Platform (Veis et al., 2006, pl. 4, fig. 17). Other similar forms from the Tonian Khastakh Formation, Siberia have been identified as *Proterocladus major* (Nagovitsin et al., 2015, figs. 9M–O), but lack branching that characterizes this taxon. Although superficially similar, we do not include these Mortensnes OWM into *Proterocladus*, a genus of early multicellular green algae, because the Mortensnes filaments are straight and lack wall thickenings (nodes) often present in the main body and the branches of *Proterocladus* (cf. Li et al., 2023, fig. 10). Morphology of thin, branching, and septate filaments is common across modern green and red algae (e.g., Leliaert et al., 2012). Although the affinity cannot be narrowed down from the present material, this complexity implies eukaryotic affinity and multicellular nature.

Unnamed Form E

Fig. 6J

cf. 2005 *Distosphaera australica*; Grey, p. 247, figs. 148A–D.

Material. Two specimens from the Mortensnes diamictite matrix.

Description. Spherical vesicles with high opacity, with numerous short, thorny processes. The processes are slightly conical and stubby. The potential outer membrane it is partially preserved, ~5 μm thick. The vesicles are 54 and 60 μm in diameter, and processes are 5–8 μm long.

Remarks. This acanthomorph is similar to *Distosphaera australica* from the early Ediacaran Tanana Formation, Australia (Grey, 2005). *Distosphaera* is characterised by short, thorny processes supporting an outer membrane. The Mortensnes specimens lack the translucent outer membrane of the Australian ones, but remnants of a membrane are present between the processes on the upper right side of the specimen (Fig. 6J). This morphotype is relatively small compared to other DPA/ECAP, including the size range of *D. australica* (64–108 μm; Grey, 2005). The high opacity and blacker colour than other OWM from the Mortensnes Formation indicate that these morphotypes might be reworked. They are not, however, observed in the underlying Nyborg assemblage.

CRediT authorship contribution statement

Heda Agić: Conceptualization, Formal analysis, Funding acquisition, Investigation, Methodology, Visualization, Writing – original draft, Writing – review & editing. **Sören Jensen:** Conceptualization, Investigation, Writing – review & editing. **Guido Meinhold:** Investigation, Writing – review & editing. **Anette E.S. Högström:** Funding acquisition, Investigation, Writing – review & editing. **Jan Ove R. Ebbestad:** Investigation, Writing – review & editing. **Magne Høyberget:**

Investigation, Writing – review & editing. **Teodoro Palacios:** Investigation. **Wendy L. Taylor:** Investigation, Writing – review & editing.

Declaration of Competing Interest

The authors declare that they have no known competing financial interests or personal relationships that could have appeared to influence the work reported in this paper.

Data availability

link to Mendeley Data will be available upon acceptance

Acknowledgements

Fieldwork was enabled by the Research Council of Norway grant 231103 to A.E.S.H. H.A. was supported by Swedish Research Council (grant VR2016-06810). Kirsti S. Moe is thanked for logistical help in the field. We are grateful to Arne Thorshøj Nielsen and Qing Tang for constructive reviews. We dedicate this paper to the memory of the fisherman Trygve Larsen who was willing to ferry geologists to remote corners of Tanafjorden.

Appendix A. Supplementary data

Supplementary data to this article can be found online at https://doi.org/10.1016/j.palaeo.2023.111956.

References

Adamson, P.W., Butterfield, N.J., 2014. Palaeobiology of a Doushantuo-type acanthomorphic acritarch assemblage from the Ediacaran Biskopås Formation, Southern Norway. Abstracts of South China 2014: A symposium and field workshop on Ediacaran and Cryogenian Stratigraphy, pp. 3–4.

Aftabi, A., Atapour, H., Mohseni, S., 2022. The Ediacaran record of glaciogenic dropstones, diamictites and cap carbonates associated with non-metamorphosed banded iron formations (BIFs) in Iran. Precambrian Res. 378 article number: 106740.

Agić, H., Cohen, P.A., 2021. Non-pollen palynomorphs in deep time: unravelling the evolution of early eukaryotes. Geol. Soc. Lond. Spec. Publ. 511, 321–342.

Agić, H., Moczydłowska, M., Yin, L., 2017. Diversity of organic-walled microfossils from the early Mesoproterozoic Ruyang Group, North China Craton–a window into the early eukaryote evolution. Precambrian Res. 297, 101–130.

Agić, H., Högström, A.E.S., Moczydłowska, M., Jensen, S., Palacios, T., Meinhold, G., Ebbestad, J.O.R., Taylor, W.L., Høyberget, M., 2019. Organically-preserved multicellular eukaryote from the early Ediacaran Nyborg Formation, Arctic Norway. Sci. Rep. 9 article number: 14659.

Agić, H., Högström, A.E.S., Jensen, S., Ebbestad, J.O.R., Vickers-Rich, P., Hall, M., Matthews, J.J., Meinhold, G., Høyberget, M., Taylor, W.L., 2022. Late Ediacaran occurrences of the organic-walled microfossils *Granomarginata* and flask-shaped *Lagoenaforma collaris* gen. et sp. nov. Geol. Mag. 159, 1071–1092.

Anderson, R.P., Macdonald, F.A., Jones, D.S., McMahon, S., Briggs, D.E., 2017. Doushantuo-type microfossils from latest Ediacaran phosphorites of northern Mongolia. Geology 45, 1079–1082.

Anesio, A.M., Laybourn-Parry, J., 2012. Glaciers and ice sheets as a biome. Trends Ecol. Evol. 27, 219–225.

Anttila, E., Macdonald, F., Bold, U., 2021. Stratigraphy of the Khuvsgul Group, Mongolia. Mongolian Geoscientist 26, 2–15. https://doi.org/10.5564/mgs.v26i52.1516.

Arvestål, E.H., Willman, S., 2020. Organic-walled microfossils in the Ediacaran of Estonia: biodiversity on the East European platform. Precambrian Res. 341 article number: 105626.

Banks, N.L., 1973. Innerelv Member: late Precambrian marine shelf deposit, east Finnmark. Nor. Geol. Unders. 288, 7–25.

Banks, N.L., Edwards, M.B., Geddes, W.P., Hobday, D.K., Reading, H.G., 1971. Late Precambrian and Cambro-Ordovician sedimentation in East Finnmark. Nor. Geol. Unders. 269, 197–236.

Batten, D.J., 1991. Reworking of plant microfossils and sedimentary provenance. In: Morton, A.C., Todd, S.P., Haughton, P.D.W. (Eds.), Developments in Sedimentary Provenance Studies, Geological Society, London, Special Publications, 57, pp. 79–90.

Berner, R.A., 1985. Sulphate reduction, organic matter decomposition and pyrite formation. Philos. Trans. Roy. Soc. London A Math. Physical Sci. 315, 25–38.

Bingen, B., Griffin, W.L., Torsvik, T.H., Saeed, A., 2005. Timing of Late Neoproterozoic glaciation on Baltica constrained by detrital zircon geochronology in the Hedmark Group, south-east Norway. Terra Nova 17, 250–258.

Boetius, A., Anesio, A.M., Deming, J.W., Mikucki, J.A., Rapp, J.Z., 2015. Microbial ecology of the cryosphere: sea ice and glacial habitats. Nat. Rev. Microbiol. 13, 677–690.

Boggiani, P.C., Gaucher, C., Sial, A.N., Babinski, M., Simon, C.M., Riccomini, C., Ferreira, V.P., Fairchild, T.R., 2010. Chemostratigraphy of the Tamengo Formation (Corumbá Group, Brazil): a contribution to the calibration of the Ediacaran carbon-isotope curve. Precambrian Res. 182, 382–401.

Bowyer, F.T., Krause, A.J., Song, Y., Huang, K.J., Fu, Y., Shen, B., Li, J., Zhu, X.K., Kipp, M.A., van Maldegem, L.M., Brocks, J.J., 2023. Biological diversification linked to environmental stabilization following the Sturtian Snowball glaciation. Sci. Adv. 9 article: eadf9999.

Brocks, J.J., Jarrett, A.J.M., Sirantoine, E., Kenig, F., Moczydłowska, M., Porter, S., Hope, J., 2016. Early sponges and toxic protists: possible sources of cryostane, an age diagnostic biomarker antedating Sturtian Snowball Earth. Geobiology 14, 129–149.

Butterfield, N.J., 2000. *Bangiomorpha pubescens* n. gen., n. sp.: implications for the evolution of sex, multicellularity, and the Mesoproterozoic/Neoproterozoic radiation of eukaryotes. Paleobiology 26, 386–404.

Cameron, K.A., Hodson, A.J., Osborn, A.M., 2012. Structure and diversity of bacterial, eukaryotic and archaeal communities in glacial cryoconite holes from the Arctic and the Antarctic. FEMS Microbiol. Ecol. 82, 254–267.

Campbell, K., Mundy, C.J., Belzile, C., Delaforge, A., Rysgaard, S., 2018. Seasonal dynamics of algal and bacterial communities in Arctic sea ice under variable snow cover. Polar Biol. 41, 41–58.

Caputo, M.V., de Melo, J.G., Streel, M., Isbell, J.L., Fielding, C.R., 2008. Late Devonian and early Carboniferous glacial records of South America. In: Fielding, C.R., Frank, T.D., Isbell, J.L. (Eds.), Resolving the Late Paleozoic Ice Age in Time and Space, Geological Society of America Special Papers, 441, pp. 161–173.

Chai, S., Hua, H., Ren, J., Dai, Q., Cui, Z., 2021. Vase-shaped microfossils from the late Ediacaran Dengying Formation of Ningqiang, South China: taxonomy, preservation and biological affinity. Precambrian Res. 352, 105968.

Chen, L., Xiao, S., Pang, K., Zhou, C., Yuan, X., 2014. Cell differentiation and germ–soma separation in Ediacaran animal embryo-like fossils. Nature 516, 238–241.

Chiglino, L., Gaucher, C., Sial, A.N., Ferreira, V.P., 2015. Acritarchs of the Ediacaran Frecheirinha Formation, Ubajara Group, northeastern Brazil. An. Acad. Bras. Cienc. 87, 635–649.

Christner, B.C., Priscu, J.C., Achberger, A.M., Barbante, C., Carter, S.P., Christianson, K., Michaud, A.B., Mikucki, J.A., Mitchell, A.C., Skidmore, M.L., Vick-Majors, T.J., 2014. A microbial ecosystem beneath the West Antarctic ice sheet. Nature 512, 310–313.

Chumakov, N.M., Pokrovsky, B.G., Melezhik, V.A., 2011. The glaciogenic Bol'Shoy Patom Formation, Lena River, central Siberia. In: Arnaud, E., Halverson, G.P., Shields-Zhou, G. (Eds.), The Geological Record of Neoproterozoic Glaciations, Geological Society of London, Memoirs, 36, pp. 309–316.

Cohen, P.A., Macdonald, F.A., 2015. The Proterozoic record of eukaryotes. Paleobiology 41, 610–632.

Cohen, P.A., Vizcaíno, M., Anderson, R.P., 2020. Oldest fossil ciliates from the Cryogenian glacial interlude reinterpreted as possible red algal spores. Palaeontology 63, 941–950.

Corkeron, M.L., George, A.D., 2001. Glacial incursion on a Neoproterozoic carbonate platform in the Kimberley region, Australia. Geol. Soc. Am. Bull. 113, 1121–1132.

Corsetti, F.A., Awramik, S.M., Pierce, D., 2003. A complex microbiota from snowball Earth times: microfossils from the Neoproterozoic Kingston Peak Formation, Death Valley, USA. Proc. Natl. Acad. Sci. 100, 4399–4404.

Cunningham, J.A., Vargas, K., Yin, Z., Bengtson, S., Donoghue, P.C., 2017. The Weng'an Biota (Doushantuo Formation): an Ediacaran window on soft-bodied and multicellular microorganisms. J. Geol. Soc. Lond. 174, 793–802.

de Oliveira, R.S., Nogueira, A.C.R., Romero, G.R., Truckenbrodt, W., da Silva Bandeira, J. C., 2019. Ediacaran ramp depositional model of the Tamengo Formation, Brazil. J. S. Am. Earth Sci. 96 article number: 102348.

Devos, N., Ingouff, M., Loppes, R., Matagne, R.F., 1998. RuBisCO adaptation to low temperatures: a comparative study in psychrophilic and mesophilic unicellular algae. J. Phycol. 34, 655–660.

Deynoux, M., Miller, J.M.G., Domack, E.W., Eyles, N., Fairchild, I., Young, G.M., 1994. Earth's Glacial Record. Cambridge University Press, Cambridge.

Ding, W., Dong, L., Sun, Y., Ma, H., Xu, Y., Yang, R., Peng, Y., Zhou, C., Shen, B., 2019. Early animal evolution and highly oxygenated seafloor niches hosted by microbial mats. Sci. Rep. 9 article number: 13628.

Domeier, M., Robert, B., Meert, J.G., Kulakov, E.V., McCausland, P.J., Trindade, R.I., Torsvik, T.H., 2023. The enduring Ediacaran paleomagnetic enigma. Earth Sci. Rev. 104444.

Ebbestad, J.O.R., Hybertsen, F., Högström, A.E.S., Jensen, S., Palacios, T., Taylor, W.L., Agić, H., Høyberget, M., Meinhold, G., 2022. Distribution and correlation of *Sabellidites cambriensis* (Annelida?) in the basal Cambrian on Baltica. Geol. Mag. 159, 1262–1283.

Edwards, M.B., 1984. Sedimentology of the Upper Proterozoic glacial record, Vestertana Group, Finnmark, North Norway. Norges Geol. Unders. Bull. 394, 1–76.

Eisenack, A., 1965. Mikrofossilien aus dem Silur Gotlands. Hystrichosphären, Problematika. [Microfossils from the Silurian of Gotland. Histrichosphaeres, Problematica]. Neues Jahrb. Geol. Palaontol. Abh. 122, 257–274 (in German).

Etemad-Saeed, N., Hosseini-Barzi, M., Adabi, M.H., Miller, N.R., Sadeghi, A., Houshmandzadeh, A., Stockli, D.F., 2016. Evidence for ca. 560 Ma Ediacaran glaciation in the Kahar formation, central Alborz Mountains, northern Iran. Gondwana Res. 31, 164–183.

Faizullin, M.Sh., 1998. New data on Baikalian microfossils of the Patom Upland. Russ. Geol. Geophys. 39, 328–337.

Farmer, J., Vidal, G., Moczydłowska, M., Strauss, H., Ahlberg, P., Siedlecka, A., 1992. Ediacaran fossils from the Innerelv Member (late Proterozoic) of the Tanafjorden area, northeastern Finnmark. Geol. Mag. 129, 181–195.

Fedonkin, M.A., 1985. Paleoikhnologiya vendskikh metazoan [Palaeontology of the Vendian metazoans]. In: Sokolov, B.S., Ivanovsky, A.B. (Eds.), Vendskaya Sistema [The Vendian System], vol. 1. Nauka, Moscow, pp. 112–117 (in Russian).
Fensome, R.A., Williams, G.L., Barss, M.S., Freeman, J.M., Hill, J.M., 1990. Acritarchs and Fossil Prasinophytes: An Index to Genera, Species and Infraspecific Taxa. In: American Association of Stratigraphic Palynologists, Contributions Series, 25, pp. 1–771.
Gehling, J.G., Droser, M.L., 2013. How well do fossil assemblages of the Ediacara Biota tell time? Geology 41, 447–450.
Germs, G.J., Knoll, A.H., Vidal, G., 1986. Latest Proterozoic microfossils from the Nama group, Namibia (south west Africa). Precambrian Res. 32, 45–62.
Gnilovskaya, M.B., 2000. Pre-Ediacaran fauna of Timan (upper Riphean annelidomorphs). Stratigr. Geol. Correl. 8, 11–39.
Golubkova, E.Y., Raevskaya, E.G., Kuznetsov, A.B., 2010. Lower Vendian microfossil assemblages of East Siberia: significance for solving regional stratigraphic problems. Stratigr. Geol. Correl. 18, 353–375.
Golubkova, E.Y., Zaitseva, T.S., Kuznetsov, A.B., Dovzhikova, E.G., Maslov, A.V., 2015. Microfossils and Rb-Sr age of glauconite in the key section of the Upper Proterozoic of the northeastern part of the Russian plate (Keltmen-1 borehole). Dokl. Earth Sci. 462, 547–551.
Grazhdankin, D., Nagovitsin, K., Golubkova, E., Karlova, G., Kochnev, B., Rogov, V., Marusin, V., 2020. Doushantuo-Pertatataka–type acanthomorphs and Ediacaran ecosystem stability. Geology 48, 708–712.
Grey, K., 1999. A modified palynological preparation technique for the extraction of large Neoproterozoic acanthomorph acritarchs and other acid-insoluble microfossils. Western Australia Geological Survey, Record 1999/10, pp. 1–23.
Grey, K., 2005. Ediacaran palynology of Australia. Memoirs Assoc. Australasian Palaeontol. 31, 1–439.
Grey, K., Calver, C.R., 2007. Correlating the Ediacaran of Australia. In: Vickers-Rich, P., Komarower, P. (Eds.), The Rise and Fall of the Ediacaran Biota, Geological Society, London, Special Publications, 286, pp. 115–135.
Grey, K., Corkeron, M., 1998. Late Neoproterozoic stromatolites in glacigenic successions of the Kimberley region, Western Australia: evidence for a younger Marinoan glaciation. Precambrian Res. 92, 65–87.
Grey, K., Willman, S., 2009. Taphonomy of Ediacaran acritarchs from Australia: significance for taxonomy and biostratigraphy. Palaios 24, 239–256.
Grey, K., Walter, M.R., Calver, C.R., 2003. Neoproterozoic biotic diversification: Snowball Earth or aftermath of the Acraman impact? Geology 31, 459–462.
Griffiths, H.J., Whittle, R.J., Mitchell, E.G., 2023. Animal survival strategies in Neoproterozoic ice worlds. Glob. Chang. Biol. 29, 10–20.
Gunia, T., 1974. Microflora prekambryjskich wapieni okolicy Dusznik Zdroju (Sudety Środkowe). [Microflora of the Precambrian limestones in the Duszniki Zdrój area (centra Sudetes).]. Ann. Soc. Geol. Pol. 44, 65–92 (in Polish).
Halverson, G.P., Hoffman, P.F., Schrag, D.P., Maloof, A.C., Rice, A.H.N., 2005. Toward a Neoproterozoic composite carbon-isotope record. GSA Bull. 117, 1181–1207.
Hamilton, T.L., Peters, J.W., Skidmore, M.L., Boyd, E.S., 2013. Molecular evidence for an active endogenous microbiome beneath glacial ice. ISME J. 7, 1402–1412.
Hancke, K., Kristiansen, S., Lund-Hansen, L.C., 2022. Highly productive ice algal mats in Arctic melt ponds: primary production and carbon turnover. Front. Mar. Sci. 9 article number: 841720.
Hannah, J., Yang, G., Bingen, B., Stein, H., Zimmerman, A., 2007. ~ 560 Ma and ~300 Ma Re-Os ages constrain Neoproterozoic glaciation and record Variscan hydrocarbon migration on extension of Oslo rift. In: Redfield, T., Buiter, S.J.H., Smethurst, M.A. (Eds.), Geodynamics, Geomagnetism and Paleogeography: A 50 Year Celebration, NGU-RAPPORT 2007.057, p. 50.
He, R., Lang, X., Shen, B., 2021. A rapid rise of seawater $\delta^{13}C$ during the deglaciation of the Marinoan Snowball Earth. Glob. Planet. Chang. 207 article number: 103672.
Hermann, T.N., 1974. On the experience of the extraction of large plant remains and microfossils using chemical dissolution of rocks. In: Microfossils of the USSR. Nauka, Novosibirsk, pp. 97–99 (in Russian).
Hoffman, P.F., 2016. Cryoconite pans on Snowball Earth: supraglacial oases for Cryogenian eukaryotes? Geobiology 14, 531–542.
Hoffman, P.F., Li, Z.X., 2009. A palaeogeographic context for Neoproterozoic glaciation. Palaeogeogr. Palaeoclimatol. Palaeoecol. 277, 158–172.
Hoffman, P.F., Abbot, D.S., Ashkenazy, Y., Benn, D.I., Brocks, J.J., Cohen, P.A., Cox, G. M., Creveling, J.R., Donnadieu, Y., Erwin, D.H., Fairchild, I.J., 2017. Snowball Earth climate dynamics and Cryogenian geology-geobiology. Sci. Adv. 3 article number: e1600983.
Högström, A.E.S., Jensen, S., Palacios, T., Ebbestad, J.O.R., 2013. New information on the Ediacaran-Cambrian transition in the Vestertana Group, Finnmark, northern Norway, from trace fossils and organic-walled microfossils. Nor. J. Geol. 93, 95–106.
Högström, A.E.S., Jensen, S., Ebbestad, J.O.R., Taylor, W.L., Høyberget, M., Agić, H., Meinhold, G., Palacios, T., 2017. Expanding the Ediacaran biota on the Digermulen Peninsula, Arctic Norway. In: Proceedings of the International Symposium on the Ediacaran-Cambrian Transition. Memorial University of Newfoundland, St Johns.
Huldtgren, T., Cunningham, J.A., Yin, C., Stampanoni, M., Marone, F., Donoghue, P.C., Bengtson, S., 2011. Fossilized nuclei and germination structures identify Ediacaran "animal embryos" as encysting protists. Science 334, 1696–1699.
Irwin, A.J., Finkel, Z.V., Schofield, O.M., Falkowski, P.G., 2006. Scaling-up from nutrient physiology to the size-structure of phytoplankton communities. J. Plankton Res. 28, 459–471.
Jachowicz-Zdanowska, M., 2011. Organic microfossil assemblages from the late Ediacaran rocks of the Małopolska Block, southeastern Poland. Geol. Quart. 55, 85–94.
Jankauskas, T.V., 1979. Lower Riphean microbiotas of the Southern Urals. Doklady Akademiya Nauk SSSR 248, 190–193 (in Russian).
Jankauskas, T.V., 1980. Shisheniakskaia mikrobiota Verkhnego Rifeia Iuzhnogo Urala (Shisheniak microbiota of the upper Riphean of the Southern Urals). Akademii Nauk SSSR. Doklady 251, 190–192 (in Russian).
Jankauskas, T.V., 1982. Microfossils from the Riphean of the Southern Urals. In: Keller, B.M. (Ed.), Stratotip rifeya: Paleontologiya, Paleomagnetizm, 368, pp. 84–120 (in Russian).
Jankauskas, T.V., Mikhailova, N.S., German, T.N., Sergeev, V.N., Abduazimova, Z.M., Velova, M.Yu, et al., 1989. Mikrofossilii dokembriya SSSR. [Precambrian microfossils of the USSR.] Trudy Instituta Geologii I Geochronologii Dokembria SSSR Akademii Nauk, Leningrad, 188 pp. (in Russian).
Jensen, S., Högström, A.E.S., Høyberget, M., Meinhold, G., McIlroy, D., Ebbestad, J.O.R., Taylor, W.L., Agić, H., Palacios, T., 2018. New occurrences of *Palaeopascichnus* from the Stáhpogieddi Formation, Arctic Norway, and their bearing on the age of the Varanger Ice Age. Can. J. Earth Sci. 55, 1253–1261.
Joshi, H., Tiwari, M., 2016. *Tianzhushania spinosa* and other large acanthomorphic acritarchs of Ediacaran Period from the Infrakrol Formation, Lesser Himalaya, India. Precambrian Res. 286, 325–336.
Kaufman, A.J., Jiang, G., Christie-Blick, N., Banerjee, D.M., Rai, V., 2006. Stable isotope record of the terminal Neoproterozoic Krol platform in the Lesser Himalayas of northern India. Precambrian Res. 147, 156–185.
Kennedy, M.J., Runnegar, B., Prave, A.R., Hoffmann, K.H., Arthur, M.A., 1998. Two or four Neoproterozoic glaciations? Geology 26, 1059–1063.
Klein, C., Beukes, N.J., Schopf, J.W., 1987. Filamentous microfossils in the early Proterozoic Transvaal Supergroup: their morphology, significance, and paleoenvironmental setting. Precambrian Res. 36, 81–94.
Knoll, A.H., 1992. Vendian microfossils in metasedimentary cherts of the Scotia Group, Prins Karls Forland, Svalbard. Palaeontology 35, 751–774.
Knoll, A.H., Swett, K., Mark, J., 1991. Paleobiology of a Neoproterozoic tidal flat/lagoonal complex: the Draken Conglomerate Formation, Spitsbergen. J. Paleontol. 65, 531–569.
Kolesnikov, A.V., Desiatkin, V., 2022. Taxonomy and palaeoenvironmental distribution of palaeopascichnids. Geol. Mag. 159, 1175–1191.
Kolesnikov, A.V., Rogov, V.I., Bykova, N.V., Danelian, T., Clausen, S., Maslov, A.V., Grazhdankin, D.V., 2018. The oldest skeletal macroscopic organism *Palaeopascichnus linearis*. Precambrian Res. 316, 24–37.
Kolosova, S.P., 1991. Pozdnedokembriyeskiye shipivatiye microfossilii vostoka Sibirskoi Platformi [Late-Precambrian thorny microfossils of the east Siberian Platform]. Algologiya 39, Yakutian Institute of Geological Sciences, Academy of Sciences, USSR, Yakutsk-91, pp. 53–59 (in Russian).
Kosiba, J., Wilk-Woźniak, E., Krztoń, W., 2019. The effect of potentially toxic cyanobacteria on ciliates (Ciliophora). Hydrobiologia 827, 325–335.
Kulling, O., 1951. Spår av Varangeristiden i Norbotten [Traces of Varanger ice age in Norrbotten]. Sveriges geologiska Undersökning A°rsbok 43 (503), 1–45 (1949). (in Swedish).
Kumpulainen, R.A., 2011. The Neoproterozoic glaciogenic Lillfjället Formation, southern Swedish Caledonides. In: Arnaud, E., Halverson, G.P., Shields-Zhou, G. (Eds.), The Geological Record of Neoproterozoic Glaciations, Geological Society, London, Memoirs, 36, pp. 629–634.
Kumpulainen, R.A., Hamilton, M.A., Söderlund, U., Nystuen, J.P., 2021. U-Pb baddeleyite age for the Ottfjället Dyke Swarm, central Scandinavian Caledonides: new constraints on Ediacaran opening of the Iapetus Ocean and glaciations on Baltica. GFF 143, 40–54.
Laybourn-Parry, J., Pearce, D., 2016. Heterotrophic bacteria in Antarctic lacustrine and glacial environments. Polar Biol. 39, 2207–2225.
Lechte, M.A., Wallace, M.W., Hood, A.V.S., Li, W., Jiang, G., Halverson, G.P., Asael, D., McColl, S.L., Planavsky, N.J., 2019. Subglacial meltwater supported aerobic marine habitats during Snowball Earth. Proc. Natl. Acad. Sci. 116, 25478–25483.
Lee, S.-J., Golubic, S., 1998. Multi-trichomous cyanobacterial microfossils from the Mesoproterozoic Gaoyuzhuang Formation, China: paleoecological and taxonomic implications. Lethaia 31, 169–184.
Lehn, I., Paim, P.S.G., Chemale Jr., F., 2022. Integrated correlation of the Camaquã Basin (Southernmost Brazil) with other Ediacaran units of southwestern Proto-Gondwana. J. S. Am. Earth Sci. 116 article number: 103812.
Leliaert, F., Smith, D.R., Moreau, H., Herron, M.D., Verbruggen, H., Delwiche, C.F., De Clerck, O., 2012. Phylogeny and molecular evolution of the green algae. Crit. Rev. Plant Sci. 31, 1–46.
Leonov, M.V., Ragozina, A.L., 2007. Upper Vendian assemblages of carbonaceous micro- and macrofossils in the White Sea Region: systematic and biostratigraphic aspects. In: Vickers-Rich, P., Komarower, P. (Eds.), The Rise and Fall of the Ediacaran Biota, Geological Society of London, Special Publication, 286, pp. 269–275.
Li, G., Pang, K., Chen, L., Zhou, G., Han, C., Yang, L., Wang, W., Yang, F., Yin, L., 2019. Organic-walled microfossils from the Tonian Tongjiazhuang Formation of the Tumen Group in western Shandong, North China Craton and their biostratigraphic significance. Gondwana Res. 76, 260–289.
Li, D., Luo, G., Tang, Q., She, Z., Xiao, S., 2023. New record of the green algal fossil Proterocladus and coexisting microfossils from the Meso-Neoproterozoic Diaoyutai Formation in southern Liaoning, North China. Precambrian Res. 393 article number: 107104.
Linnemann, U., Hofmann, M., Gärtner, A., Gärtner, J., Zieger, J., Krause, R., Haenel, R., Mende, K., Ovtcharova, M., Schaltegger, U., Vickers-Rich, P., 2022. An Upper Ediacaran Glacial Period in Cadomia: the Granville tillite (Armorican Massif)–sedimentology, geochronology and provenance. Geol. Mag. 159, 999–1013.
Liu, P., Moczydłowska, M., 2019. Ediacaran microfossils from the Doushantuo Formation chert nodules in the Yangtze Gorges area, South China, and new biozones. Fossils Strata 65, 1–172. https://doi.org/10.1002/9781119564225.ch1.

Liu, P., Yin, C., Chen, S., Tang, F., Gao, L., 2013. The biostratigraphic succession of acanthomorphic acritarchs of the Ediacaran Doushantuo Formation in the Yangtze Gorges area, South China and its biostratigraphic correlation with Australia. Precambrian Res. 225, 29–43.
Liu, P., Chen, S., Zhu, M., Li, M., Yin, C., Shang, X., 2014. High-resolution biostratigraphic and chemostratigraphic data from the Chenjiayuanzi section of the Doushantuo Formation in the Yangtze Gorges area, South China: implication for subdivision and global correlation of the Ediacaran System. Precambrian Res. 249, 199–214.
Manning-Berg, A.R., Wood, R.S., Williford, K.H., Czaja, A.D., Kah, L.C., 2019. The taphonomy of Proterozoic microbial mats and implications for early diagenetic silicification. Geosciences 9 article number: 40.
Marshall, J.E.A., 1991. Quantitative spore colour. J. Geol. Soc. Lond. 148, 223–233.
McGee, B., Collins, A.S., Trindade, R.I., 2013. A glacially incised canyon in Brazil: further evidence for mid-Ediacaran glaciation? J. Geol. 121, 275–287.
McIlroy, D., Brasier, M.D., 2017. Ichnological evidence for the Cambrian explosion in the Ediacaran to Cambrian succession of Tanafjord, Finnmark, northern Norway. In: Brasier, A.T., McIlroy, D., McLoughlin, N. (Eds.), Earth System Evolution and Early.
Mehrotra, N.C., Babu, R., Tewari, R., Jha, N., Kumar, P., Singh, V.K., Shukla, M., 2008. New global opportunities for hydrocarbon exploration in Neoproterozoic basins of Indian Subcontinent. J. Geol. Soc. India 72, 543–546.
Meinhold, G., Jensen, S., Høyberget, M., Arslan, A., Ebbestad, J.O.R., Högström, A.E.S., Palacios, T., Agić, H., Taylor, W.L., 2019a. First record of carbonates with spherulites and cone-in-cone structures from the Precambrian of Arctic Norway, and their palaeoenvironmental significance. Precambrian Res. 328, 99–110.
Meinhold, G., Wemmer, K., Högström, A.E.S., Ebbestad, J.O.R., Jensen, S., Palacios, T., Høyberget, M., Agić, H., Taylor, W.L., 2019b. A late Caledonian tectono-thermal event in the Gaissa Nappe Complex, Arctic Norway: fine-fraction K-Ar evidence from the Digermulen Peninsula. GFF 141, 289–294.
Meinhold, G., Willbold, M., Karius, V., Jensen, S., Agić, H., Ebbestad, J.O.R., Palacios, T., Högström, A.E.S., Høyberget, M., Taylor, W.L., 2022. Rare earth elements and neodymium and strontium isotopic constraints on provenance switch and post-depositional alteration of fossiliferous Ediacaran and lowermost Cambrian strata from Arctic Norway. Precambrian Res. 381 article number: 106845.
Merdith, A.S., Collins, A.S., Williams, S.E., Pisarevsky, S., Foden, J.D., Archibald, D.B., Blades, M.L., Alessio, B.L., Armistead, S., Plavsa, D., Clark, C., 2017. A full-plate global reconstruction of the Neoproterozoic. Gondwana Res. 50, 84–134.
Merdith, A.S., Williams, S.E., Collins, A.S., Tetley, M.G., Mulder, J.A., Blades, M.L., Young, A., Armistead, S.E., Cannon, J., Zahirovic, S., Müller, R.D., 2021. Extending full-plate tectonic models into deep time: linking the Neoproterozoic and the Phanerozoic. Earth Sci. Rev. 214 article number: 103477.
Mertens, K.N., Ribeiro, S., Bouimetarhan, I., Caner, H., Nebout, N.C., Dale, B., De Vernal, A., Ellegaard, M., Filipova, M., Godhe, A., Goubert, E., 2009. Process length variation in cysts of a dinoflagellate, *Lingulodinium machaerophorum*, in surface sediments: investigating its potential as salinity proxy. Mar. Micropaleontol. 70, 54–69.
Millikin, A.E., Strauss, J.V., Halverson, G.P., Bergmann, K.D., Tosca, N.J., Rooney, A.D., 2022. Calibrating the Russøya excursion in Svalbard, Norway, and implications for Neoproterozoic chronology. Geology 50, 506–510.
Moczydłowska, M., 2008. The Ediacaran microbiota and the survival of Snowball Earth conditions. Precambrian Res. 167, 1–15.
Moczydłowska, M., 2016. Algal affinities of Ediacaran and Cambrian organic-walled microfossils with internal reproductive bodies: *Tanarium* and other morphotypes. Palynology 40, 83–121.
Moczydłowska, M., Nagovitsin, K.E., 2012. Ediacaran radiation of organic-walled microbiota recorded in the Ura Formation, Patom Uplift, East Siberia. Precambrian Res. 198, 1–24.
Moczydłowska, M., Vidal, G., Rudavskaya, V.A., 1993. Neoproterozoic (Vendian) phytoplankton from the Siberian platform, Yakutia. Palaeontology 36, 495–521.
Moczydłowska, M., Pease, V., Willman, S., Wickström, L., Agić, H., 2018. A Tonian age for the Visingsö Group in Sweden constrained by detrital zircon dating and biochronology: implications for evolutionary events. Geol. Mag. 155, 1175–1189.
Morais, L., Fairchild, T.R., Freitas, B.T., Rudnitzki, I.D., Silva, E.P., Lahr, D., Moreira, A. C., Abrahão Filho, E.A., Leme, J.M., Trindade, R.I.F., 2022. Doushantuo-Pertatataka—Like Acritarchs from the Late Ediacaran Bocaina Formation (Corumbá Group, Brazil). Front. Earth Sci. 9 https://doi.org/10.3389/feart.2021.787011 article number: 787011.
Nagovitsin, K.E., Rogov, V.I., Marusin, V.V., Karlova, G.A., Kolesnikov, A.V., Bykova, N. V., Grazhdankin, D.V., 2015. Revised Neoproterozoic and Terreneuvian stratigraphy of the Lena-Anabar Basin and north-western slope of the Olenek Uplift. Siberian Platform. Precambrian Res. 270, 226–245.
Naumova, S.N., 1949. Spory nizhnego kembriya. [Spores from the lower Cambrian]. Izvestiya Akademii Nauk SSSR, Seriya Geologicheskaya 4, 49–56 (in Russian).
Nystuen, J.P., 1976. Late Precambrian Moelv tillite deposited on a discontinuity surface associated with a fossil ice wedge, Rendalen, southern Norway. Nor. Geol. Tidsskr. 56, 29–50.
Nystuen, J.P., 1985. Facies and preservation of glaciogenic sequences from the Varanger ice age in Scandinavia and other parts of the North Atlantic region. Palaeogeogr. Palaeoclimatol. Palaeoecol. 51, 209–229.
Nystuen, J.P., Andresen, A., Kumpulainen, R.A., Siedlecka, A., 2008. Neoproterozoic basin evolution in Fennoscandia, East Greenland and Svalbard. Episodes 31, 35–43.
Ouyang, Q., Guan, C., Zhou, C., Xiao, S., 2017. Acanthomorphic acritarchs of the Doushantuo Formation from an upper slope section in northwestern Hunan Province, South China, with implications for early–middle Ediacaran biostratigraphy. Precambrian Res. 298, 512–529.
Parry, L.A., Boggiani, P.C., Condon, D.J., Garwood, R.J., Leme, J.D.M., McIlroy, D., Brasier, M.D., Trindade, R., Campanha, G.A., Pacheco, M.L., Diniz, C.Q., 2017. Ichnological evidence for meiofaunal bilaterians from the terminal Ediacaran and earliest Cambrian of Brazil. Nat. Ecol. Evol. 1, 1455–1464.
Pehr, K., Love, G.D., Kuznetsov, A., Podkovyrov, V., Junium, C.K., Shumlyanskyy, L., Sokur, T., Bekker, A., 2018. Ediacara biota flourished in oligotrophic and bacterially dominated marine environments across Baltica. Nat. Commun. 9, 1807.
Pokrovskii, B.G., Melezhik, V.A., Bujakaite, M.I., 2006. Carbon, oxygen, strontium, and sulfur isotopic compositions in late Precambrian rocks of the Patom Complex, Central Siberia: communication 2. Nature of carbonates with ultralow and ultrahigh.
Porter, S.M., Riedman, L.A., 2016. Systematics of organic-walled microfossils from the ~780–740 Ma Chuar Group, Grand Canyon, Arizona. J. Paleontol. 40, 815–853.
Prasad, B., Asher, R., 2001. Acritarch biostratigraphy and lithostratigraphic classification of Proterozoic and Lower Paleozoic sediments (preunconformity sequence) of Ganga Basin, India. Paleontogr. Indica 5, 1–151.
Prasad, B., Asher, R., 2016. Record of Ediacaran complex acanthomorphic acritarchs from the Lower Vindhyan succession of the Chambal Valley (east Rajasthan), India and their biostratigraphic significance. J. Palaeontol. Soc. India 61, 29–62.
Prasad, B., Asher, R., Borgohai, B., 2010. Late Neoproterozoic (Ediacaran)-Early Paleozoic (Cambrian) acritarchs from the Marwar Supergroup, Bikaner-Nagaur Basin, Rajasthan. J. Geol. Soc. India 75, 415–431.
Preußel, K., Wessel, G., Fastner, J., Chorus, I., 2009. Response of cylindrospermopsin production and release in *Aphanizomenon flos-aquae* (Cyanobacteria) to varying light and temperature conditions. Harmful Algae 8, 645–650.
Pu, J.P., Bowring, S.A., Ramezani, J., Myrow, P., Raub, T.D., Landing, E., Mills, A., Hodgin, E., Macdonald, F.A., 2016. Dodging snowballs: geochronology of the Gaskiers glaciation and the first appearance of the Ediacaran biota. Geology 44, 955–958.
Pyatiletov, V.G., 1978. Mikrofossilii Manskogo progiba (Microfossils of the Mansk Trough). In: Geologicheskoe Stroenie Manskogo Progiba i Ego Poloshenie Sayano-Altaiskikh "Baikalidakh" (Geological Constitution of Mansk Trough and its position in the Sayan-Altai "Baikalides"). Akad. Nauk SSSR, Sibirskoe Otdelenie, Institut Geologii i Geofiziki, Novosibirsk, Trudy 400, pp. 175–211 (in Russian).
Reading, H.G., 1965. Eocambrian and Lower Palaeozoic geology of the Digermul Peninsula, Tanafjord, Finnmark. Nor. Geol. Unders. 234, 167–191.
Reading, H.G., Walker, R.G., 1966. Sedimentation of Eocambrian tillites and associated sediments in Finnmark, northern Norway. Palaeogeogr. Palaeoclimatol. Palaeoecol. 2, 177–212.
Reinl, K.L., Harris, T.D., North, R.L., Almela, P., Berger, S.A., Bizic, M., Burnet, S.H., Grossart, H., Ibelings, B.W., Jakobsson, E., Knoll, L.B., Lafrancois, B.M., McElarney, Y., Morales-Williams, A.M., Obertegger, U., Ogashawara, I., Paule-Mercado, C., Peierls, B.L., Rusak, J.A., Sarkar, S., Sharma, S., Trout-Haney, J.V., Urrutia-Cordero, P., Vankiteswaran, J.J., Wain, D.J., Warner, K., Weyhenmeyer, G. A., Yokota, K., 2023. Blooms also like it cold. Limnol. Oceanogr. Lett. 8, 546–564.
Rice, A.H.N., 1994. Stratigraphic overlap of the late Proterozoic Vadsø and Barents Sea Groups and correlation across the Trollfjorden-Komagelva Fault, Finnmark, North Norway. Nor. Geol. Tidsskr. 74, 48–57.
Rice, A.H.N., 2023. U-Pb baddeleyite age for the Ottfjället Dyke Swarm, central Scandinavian Caledonides: new constraints on Ediacaran opening of the Iapetus Ocean and glaciations on Baltica – a comment on the inferred age of Neoproterozoic glaciations. GFF. https://doi.org/10.1080/11035897.2023.2205893.
Rice, A.H.N., Hofmann, C., Pettersen, A., 2001. A new sedimentary succession from the southern margin of the Neoproterozoic Gaissa Basin, south Varangerfjord, North Norway; the Lattanjar'ga unit. Nor. J. Geol. 81, 41–48.
Rice, A.H.N., Edwards, M.B., Hansen, T.A., Arnaud, E., Halverson, G.P., 2011. Glaciogenic rocks of the Neoproterozoic Smalfjord and Mortensnes formations, Vestertana Group, E. Finnmark, Norway. In: Arnaud, E., Halverson, G.P., Shields-Zhou, G. (Eds.), The Geological Record of Neoproterozoic Glaciations, Memoirs 36. Geological Society, London, pp. 593–602.
Rice, A.H.N., Edwards, M.B., Hansen, T.A., 2012. Neoproterozoic glacial and associated facies in the Tanafjord-Varangerfjord area, Finnmark, north Norway. In: Geological Society of America, Field Guide 26, Vol. 26, pp. 1–78.
Riedman, L.A., Porter, S.M., Halverson, G.P., Hurtgen, M.T., Junium, C.K., 2014. Organic-walled microfossil assemblages from glacial and interglacial Neoproterozoic units of Australia and Svalbard. Geology 42, 1011–1014.
Roberts, D., Gee, D.G., 1985. An introduction to the structure of the Scandinavian Caledonides. In: Gee, D.G., Stuart, B.A. (Eds.), The Caledonide Orogen – Scandinavia and Related Areas. John Wiley & Sons, Chichester, pp. 55–68.
Roberts, D., Siedlecka, A., 2022. Revised stratigraphy and correlation of the Neoproterozoic successions of Varanger Peninsula, East Finnmark, northern Norway, and the Rybachi–Sredni peninsulas and Kildin Island in Northwest Russia. Norges Geol. Unders. Bull. 457, 1–21.
Rooney, A.D., Strauss, J.V., Brandon, A.D., Macdonald, F.A., 2015. A Cryogenian chronology: two long-lasting synchronous Neoproterozoic glaciations. Geology 43, 459–462.
Rooney, A.D., Cantine, M.D., Bergmann, K.D., Gómez-Pérez, I., Al Baloushi, B., Boag, T. H., Busch, J.F., Sperling, E.A., Strauss, J.V., 2020. Calibrating the coevolution of Ediacaran life and environment. Proc. Natl. Acad. Sci. 117, 16824–16830.
Rowland, S.M., Rodriguez, M.G., 2014. A multicellular alga with exceptional preservation from the Ediacaran of Nevada. J. Paleontol. 88, 263–268.
Rud'ko, S.V., Kuznetsov, A.B., Petrov, P.Y., Sitkina, D.R., Kaurova, O.K., 2021. Pb-Pb dating of the Dal'nyaya Taiga Group in the Ura uplift of southern Siberia: implications for correlation of C-isotopic and biotic events in the Ediacaran. Precambrian Res. 362 article number: 106285.
Sabouri, J., Frahani, B., Narimani, H., 2003. Discovery of index microfossil *Cochleatina* from the top of the Kahar Formation in Firooz-Abad section of Chalus and analysis of

the age of this formation in Iran. In: Proceedings of the 21th Symposium on Geosciences. Geological Survey of Iran. (in Persian).
Schopf, J.W., 1968. Microflora of the Bitter Springs formation, late Precambrian, central Australia. J. Paleontol. 42, 651–688.
Sergeev, V.N., Knoll, A.H., Vorob'eva, N.G., 2011. Ediacaran microfossils from the Ura Formation, Baikal-Patom Uplift, Siberia: taxonomy and biostratigraphic significance. J. Paleontol. 85, 987–1011.
Sergeev, V.N., Vorob'eva, N.G., Petrov, P.Y., 2017. The biostratigraphic conundrum of Siberia: do true Tonian–Cryogenian microfossils occur in Mesoproterozoic rocks? Precambrian Res. 299, 282–302.
Sforna, M.C., Loron, C.C., Demoulin, C.F., François, C., Cornet, Y., Lara, Y.J., Grolimund, D., Ferreira Sanchez, D., Medjoubi, K., Somogyi, A., Addad, A., Compère, P., Baudet, D., Brocks, J.J., Javaux, E.J., 2022. Intracellular bound chlorophyll residues identify 1 Gyr-old fossils as eukaryotic algae. Nat. Commun. 13 article number: 146.
Sharma, M., Shukla, Y., Sergeev, V.N., 2021. Microfossils from the Krol 'A' of the Lesser Himalaya, India: additional supporting data for its early Ediacaran age. Palaeoworld 30, 610–626.
Shen, B., Xiao, S., Zhou, C., Kaufman, A.J., Yuan, X., 2010. Carbon and sulfur isotope chemostratigraphy of the Neoproterozoic Quanji Group of the Chaidam Basin, NW China: basin stratification in the aftermath of an Ediacaran glaciation postdating the Shuram event? Precambrian Res. 177, 241–252.
Shukla, R., Tiwari, M., 2014. Ediacaran acanthomorphic acritarchs from the Outer Krol Belt, Lesser Himalaya, India: their significance for global correlation. Palaeoworld 23, 209–224.
Siedlecka, A., Siedlecki, S., 1971. Late Precambrian sedimentary rocks of the Tanafjord-Varangerfjord region of Varanger Peninsula, northern Norway. Nor. Geol. Unders. 269, 246–294.
Siedlecka, A., Reading, H.G., Williams, G.D., Roberts, D., 2006. Langfjorden, Preliminary Bedrock Geology Map 2236 II, Scale 1:50000. Norges Geologiske Undersøkelse, Trondheim.
Slater, B.J., Harvey, T.H., Bekker, A., Butterfield, N.J., 2020. *Cochleatina*: an enigmatic Ediacaran–Cambrian survivor among small carbonaceous fossils (SCFs). Palaeontology 63, 733–752.
Soldatenko, Y., El Albani, A., Ruzina, M., Fontaine, C., Nesterovsky, V., Paquette, J.L., Meunier, A., Ovtcharova, M., 2019. Precise U-Pb age constrains on the Ediacaran biota in Podolia, East European Platform, Ukraine. Sci. Rep. 9 article number: 1675.
Spjeldnæs, N., 1963. A new fossil (*Papillomembrana* sp.) from the Upper Precambrian of Norway. Nature 200, 63–64.
Spjeldnæs, N., 1967. Fossils from pebbles in the Biskopåsen Formation in Southern Norway. Nor. Geol. Unders. 251, 53–83.
Środoń, J., Condon, D.J., Golubkova, E., Millar, I.L., Kuzmenkova, O., Paszkowski, M., Mazur, S., Kędzior, A., Drygant, D., Ciobotaru, V., Liivamägi, S., 2023. Ages of the Ediacaran Volyn-Brest trap volcanism, glaciations, paleosols, Podillya Ediacaran soft-bodied organisms, and the Redkino-Kotlin boundary (East European Craton) constrained by zircon single grain U-Pb dating. Precambrian Res. 386 article number: 106962.
Staplin, F.L., 1969. Sedimentary organic matter, organic metamorphism, and oil and gas occurrence. Bull. Can. Petrol. Geol. 17, 47–66.
Streel, M., Caputo, M.V., Loboziak, S., Melo, J.H., Thorez, J., 2001. Palynology and sedimentology of laminites and tillites from the latest Famennian of the Parnaíba Basin, Brazil. Geol. Belg. 3, 87–96.
Tang, Q., Pang, K., Yuan, X., Wan, B., Xiao, S., 2015. Organic-walled microfossils from the Tonian Gouhou Formation, Huaibei region, North China Craton, and their biostratigraphic implications. Precambrian Res. 266, 296–318.
Thierstein, H.R., Macdougall, J.D., Martin, E.E., Larsen, B., Barron, J., Baldauf, J., 1991. Age determinations of Paleogene diamictites from Prydz Bay (Site 739), Antarctica, using Sr isotopes of molluscs and biostratigraphy of microfossils (diatoms and coccoliths). In: Barron, J., Larsen, B., et al. (Eds.), Proceedings of the Ocean Drilling Program, Scientific Results, 119, pp. 739–745.
Timofeev, B.V., 1966. Micropaleophytological research into ancient strata. [Mikropaleofitologicheskoe issledovanie drevnykh svit]. Akademiya Nauk SSSR, Nauka 89, pp. 1–126 (in Russian).
Timofeev, B.V., Hermann, T.N., Mikhailova, N.S., 1976. Mikrofitofossilii dokembria, kembria i ordovika (Microphytofossils of the Precambrian, Cambrian and Ordovician). Nauka, Leningrad, 106 p. (in Russian).
Tostevin, R., Mills, B.J., 2020. Reconciling proxy records and models of Earth's oxygenation during the Neoproterozoic and Palaeozoic. Interface Focus 10 article 20190137.
Van Cappellen, P., Ingall, E.D., 1994. Benthic phosphorus regeneration, net primary production, and ocean anoxia: a model of the coupled marine biogeochemical cycles of carbon and phosphorus. Paleoceanography 9, 677–692.
Veis, A.F., Vorob'eva, N.G., Golubkova, E.Y., 2006. The early Vendian microfossils first found in the Russian Plate: taxonomic composition and biostratigraphic significance. Stratigr. Geol. Correl. 14, 368–385.
Vidal, G., 1976. Late Precambrian acritarchs from the Eleonore Bay group and Tillite group in East Greenland. Rapp. Grønl. Geol. Unders. 78, 1–19.
Vidal, G., 1981. Micropalaeontology and biostratigraphy of the Upper Proterozoic and Lower Cambrian sequence in East Finnmark, Northern Norway. Norges Geol. Unders. Bull. 362, 1–53.
Vidal, G., 1990. Giant acanthomorph acritarchs from the upper Proterozoic in southern Norway. Palaeontology 33, 287–298.
Vidal, G., Siedlecka, A., 1983. Planktonic, acid-resistant microfossils from the Upper Proterozoic strata of the Barents Sea region of Varanger Peninsula, East Finnmark, northern Norway. Nor. Geol. Unders. 382, 45–79.
Vincent, W.F., Gibson, J.A.E., Pienitz, R., Villeneuve, V., Broady, P.A., Hamilton, P.B., Howard-Williams, C., 2000. Ice shelf microbial ecosystems in the High Arctic and implications for life on Snowball Earth. Naturwissenschaften 87, 137–141.
Volkova, N.A., Kirjanov, V.V., Piskun, L.V., Paskeviciene, L.T., Jankauskas, T.V., 1983. Plant microfossils. In: Urbanek, A., Rozanov, A.Yu. (Eds.), Upper Precambrian and Cambrian Palaeontology of the East-European Platform. Wydawnictwa Geologiczne, Warsaw, pp. 7–46.
Vorob'eva, N.G., Petrov, P.Y., 2020. Microbiota of the Barakun Formation and biostratigraphic characteristics of the Dal'nyaya Taiga Group: early Vendian of the Ura Uplift (Eastern Siberia). Stratigr. Geol. Correl. 28, 365–380.
Vorob'eva, N.G., Sergeev, V.N., Chumakov, N.M., 2008. New finds of early Vendian microfossils in the Ura Formation: revision of the Patom Supergroup age, Middle Siberia. Dokl. Earth Sci. 419, 411–416.
Vorob'eva, N.G., Sergeev, V.N., Knoll, A.H., 2009. Neoproterozoic microfossils from the northeastern margin of the East European Platform. J. Paleontol. 83, 161–196.
Wang, R., Shen, B., Lang, X., Wen, B., Mitchell, R.N., Ma, H., Yin, Z., Peng, Y., Liu, Y., Zhou, C., 2023. A Great late Ediacaran ice age. Natl. Sci. Rev. 10 article number: nwad117.
Ward, B.A., Dutkiewicz, S., Follows, M.J., 2014. Modelling spatial and temporal patterns in size-structured marine plankton communities: top–down and bottom–up controls. J. Plankton Res. 36, 31–47.
Willman, S., Moczydłowska, M., 2008. Ediacaran acritarch biota from the Giles 1 drillhole, Officer Basin, Australia, and its potential for biostratigraphic correlation. Precambrian Res. 162, 498–530.
Willman, S., Slater, B.J., 2021. Late Ediacaran organic microfossils from Finland. Geol. Mag. 158, 2231–2244.
Willman, S., Moczydłowska, M., Grey, K., 2006. Neoproterozoic (Ediacaran) diversification of acritarchs—a new record from the Murnaroo 1 drillcore, eastern Officer Basin, Australia. Rev. Palaeobot. Palynol. 139, 17–39.
Xiao, S., 2004. Neoproterozoic glaciations and the fossil record. In: Jenkins, G.S., McMenamin, M.A.S., McKey, C.P., Sohl, L. (Eds.), The Extreme Proterozoic: Geology, Geochemistry, and Climate, 146, pp. 199–214.
Xiao, S., Narbonne, G.M., 2020. The Ediacaran Period. In: Gradstein, F.M., Ogg, J.G., Schmitz, M.D., Ogg, G.M. (Eds.), Geologic Time Scale 2020, Vol. 1. Elsevier, pp. 521–561.
Xiao, S., Yuan, X., Steiner, M., Knoll, A.H., 2002. Macroscopic carbonaceous compressions in a terminal Proterozoic shale: a systematic reassessment of the Miaohe biota, South China. J. Paleontol. 76, 347–376.
Xiao, S., Zhou, C., Liu, P., Wang, D., Yuan, X., 2014a. Phosphatized acanthomorphic acritarchs and related microfossils from the Ediacaran Doushantuo Formation at Weng'an (South China) and their implications for biostratigraphic correlation. J. Paleontol. 88, 1–67.
Xiao, S., Muscente, A.D., Chen, L., Zhou, C., Schiffbauer, J.D., Wood, A.D., Polys, N.F., Yuan, X., 2014b. The Weng'an biota and the Ediacaran radiation of multicellular eukaryotes. Natl. Sci. Rev. 1, 498–520.
Xiao, S., Narbonne, G.M., Zhou, C., Laflamme, M., Grazhdankin, D.V., Moczydłowska-Vidal, M., Cui, H., 2016. Towards an Ediacaran time scale: problems, protocols, and prospects. Episodes 39, 540–555.
Xiao, S., Jiang, G., Ye, Q., Ouyang, Q., Banerjee, D.M., Singh, B.P., Muscente, A.D., Zhou, C., Hughes, N.C., 2022. Systematic paleontology, acritarch biostratigraphy, and $\delta^{13}C$ chemostratigraphy of the early Ediacaran Krol A Formation, Lesser Himalaya, northern India. J. Paleontol. https://doi.org/10.1017/jpa.2022.7.
Yan, Y., 1982. *Schizofusa* from the Chuanlinggou Formation of Changcheng System in Jixian County. Bull. Tianjin Inst. Geol. Mineral Resourc. Chinese Acad. Geol. Sci. 6, 1–7 (in Chinese).
Yang, C., Rooney, A.D., Condon, D.J., Li, X.H., Grazhdankin, D.V., Bowyer, F.T., Hu, C., Macdonald, F.A., Zhu, M., 2021. The tempo of Ediacaran evolution. Sci. Adv. 7 article number: eabi9643.
Ye, Q., Tong, J., Xiao, S., Zhu, S., An, Z., Tian, L., Hu, J., 2015. The survival of benthic macroscopic phototrophs on a Neoproterozoic Snowball Earth. Geology 43, 507–510.
Ye, Y., Shen, J., Feng, Q., Lash, G.G., 2020. Microbial and animal evolution in relation to redox fluctuations in a deep-water setting of South China during the Ediacaran-Cambrian transition (ca. 551–523 Ma). Palaeogeogr. Palaeoclimatol. Palaeoecol. 546 article number: 109672.
Ye, Q., Li, J., Tong, J., An, Z., Hu, J., Xiao, S., 2022. A microfossil assemblage from the Ediacaran Doushantuo Formation in the Shennongjia area (Hubei Province, South China): filling critical paleoenvironmental and biostratigraphic gaps. Precambrian Res. 377 article number: 106691.
Ye, Q., An, Z., Yu, Y., Zhou, Z., Hu, J., Tong, J., Xiao, S., 2023. Phosphatized microfossils from the Miaohe Member of South China and their implications for the terminal Ediacaran biodiversity decline. Precambrian Res. 388 article number: 107001.
Yin, L., Yuan, X., 2007. Radiation of Meso-Neoproterozoic and early Cambrian protists inferred from the microfossil record of China. Palaeogeogr. Palaeoclimatol. Palaeoecol. 254, 350–361.
Yin, L.M., Wang, D., Yuan, X.L., Zhou, C.M., 2011. Diverse small spinose acritarchs from the Ediacaran Doushantuo Formation, South China. Palaeoworld 20, 279–289.
Yuan, X., Hofmann, H.J., 1998. New microfossils from the Neoproterozoic (Sinian) Doushantuo Formation, Wengan, Guizhou Province, southwestern China. Alcheringa 22, 189–222.
Yuan, X., Chen, Z., Xiao, S., Zhou, C., Hua, H., 2011. An early Ediacaran assemblage of macroscopic and morphologically differentiated eukaryotes. Nature 470, 390–393.
Zang, Z.W., Walter, M.R., 1992. Late Proterozoic and Cambrian microfossils and biostratigraphy, Amadeus basin, central Australia. Assoc. Australasian Palaeontol. Memoir 12, 1–132.

Zhang, Y., Yin, L., Xiao, S., Knoll, A.H., 1998. Permineralized fossils from the terminal Proterozoic Doushantuo Formation, south China. Paleontol. Soc. Memoir 50, 1–52.
Zhang, S., Jiang, G., Han, Y., 2008. The age of the Nantuo Formation and Nantuo glaciation in South China. Terra Nova 20, 289–294.
Zhang, H., Sun, Y., Zeng, Q., Crowe, S.A., Luo, H., 2021. Snowball Earth, population bottleneck and *Prochlorococcus* evolution. Proc. R. Soc. B 288 article number: 20211956.
Zhou, C., Brasier, M.D., Xue, Y., 2001. Three-dimensional phosphatic preservation of giant acritarchs from the terminal Proterozoic Doushantuo Formation in Guizhou and Hubei provinces, South China. Palaeontology 44, 1157–1178.
Zhou, C., Xie, G., McFadden, K., Xiao, S., Yuan, X., 2007. The diversification and extinction of Doushantuo-Pertatataka acritarchs in South China: causes and biostratigraphic significance. Geol. J. 42, 229–262.
Zumberge, J.A., Love, G.D., Cárdenas, P., Sperling, E.A., Gunasekera, S., Rohrssen, M., Grosjean, E., Grotzinger, J.P., Summons, R.E., 2018. Demosponge steroid biomarker 26-methylstigmastane provides evidence for Neoproterozoic animals. Nat. Ecol. Evol. 2, 1709–1714.